AD-A183 676 AUTOREGRESSIVE METHODS FOR SPECTRAL ESTIMATION FROM INTERFEROGRAMS..(U) UTAH STATE UNIV LOGAN CENTER FOR SPACE ENGINEERING E N RICHARDS ET AL. 19 SEP 86 1/1

UNCLASSIFIED CSE/86-106 AGGL-TR-87-0008 F19628-83-C-0056 F/G 20/6 NL

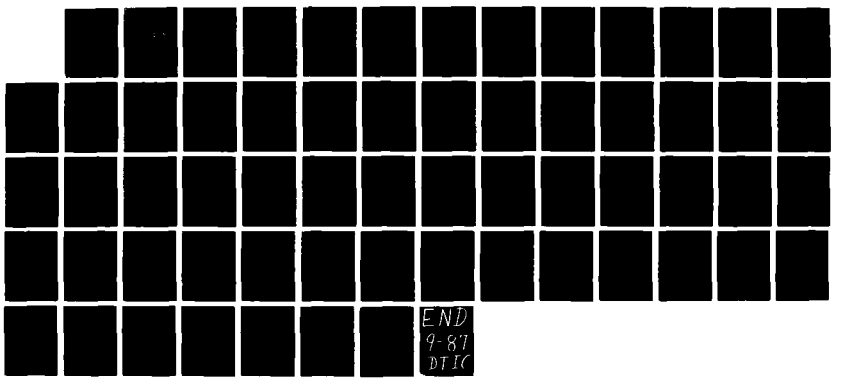

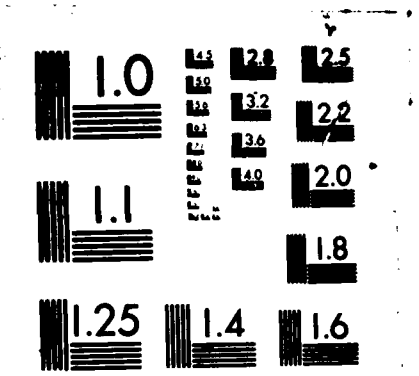

(12)

AFGL-TR-87-0008

AUTOREGRESSIVE METHODS FOR SPECTRAL ESTIMATION FROM INTERFEROGRAMS

Edward N. Richards
Susan H. Delay
William F. Grieder

Boston College
Space Data Analysis Laboratory
Chestnut Hill, MA 02167

The work reported herein was
performed under subcontract to
Center for Space Engineering
Utah State University
Logan, UT 84322-4140

Scientific Report No. 17
AFGL Contract No. F19628-83-C-0056

19 September 1986

AIR FORCE GEOPHYSICS LABORATORY
AIR FORCE SYSTEMS COMMAND
UNITED STATES AIR FORCE
HANSCOM AIR FORCE BASE
MASSACHUSETTS 01731

"This technical report has been reviewed and is approved for publication"

(Signature)
FRANCIS X. ROBERT
Contract Manager

(Signature)
RANDALL E. MURPHY, Acting Chief
Atmospheric Backgrounds Branch

FOR THE COMMANDER

(Signature)
RANDALL E. MURPHY, Director
Infrared Technology Division

This report has been reviewed by the ESD Public Affairs Office (PA) and is releasable to the National Technical Information Service (NTIS).

Qualified requestors may obtain additional copies from the Defense Technical Information Center. All others should apply to the National Technical Information Service.

If your address has changed, or if you wish to be removed from the mailing list, or if the addressee is no longer employed by your organization, please notify AFGL/DAA, Hanscom AFB, MA 01731. This will assist us in maintaining a current mailing list.

Do not return copies of this report unless contractual obligations or notices on a specific document requires that it be returned.

Unclassified

SECURITY CLASSIFICATION OF THIS PAGE

REPORT DOCUMENTATION PAGE

1a. REPORT SECURITY CLASSIFICATION: Unclassified	1b. RESTRICTIVE MARKINGS
2a. SECURITY CLASSIFICATION AUTHORITY	3. DISTRIBUTION/AVAILABILITY OF REPORT: Approved for public release; distribution unlimited.
2b. DECLASSIFICATION/DOWNGRADING SCHEDULE	
4. PERFORMING ORGANIZATION REPORT NUMBER(S): CSE/86-106	5. MONITORING ORGANIZATION REPORT NUMBER(S): AFGL-TR-87-0008
6a. NAME OF PERFORMING ORGANIZATION: Center for Space Engineering; 6b. OFFICE SYMBOL (If applicable):	7a. NAME OF MONITORING ORGANIZATION: Air Force Geophysics Laboratory
6c. ADDRESS (City, State and ZIP Code): Utah State University, Logan, UT 84322-4140	7b. ADDRESS (City, State and ZIP Code): Hanscom Air Force Base, Bedford, MA 01731
8a. NAME OF FUNDING/SPONSORING ORGANIZATION: Air Force Geophysics Laboratory; 8b. OFFICE SYMBOL (If applicable): LS	9. PROCUREMENT INSTRUMENT IDENTIFICATION NUMBER: F19628-83-C-0056
8c. ADDRESS (City, State and ZIP Code): Hanscom Air Force Base, Bedford, MA 01731	10. SOURCE OF FUNDING NOS.

PROGRAM ELEMENT NO.	PROJECT NO.	TASK NO.	WORK UNIT NO.
62101F	7670	10	AK

11. TITLE (Include Security Classification): AR Methods for Spectral Estimation from (cont)

12. PERSONAL AUTHOR(S): Edward N. Richards, Susan H. Delay, William F. Grieder

13a. TYPE OF REPORT	13b. TIME COVERED	14. DATE OF REPORT (Yr., Mo., Day)	15. PAGE COUNT
Scientific Rep. No. 17	FROM 10/1/84 TO 9/30/85	86/09/19	60

16. SUPPLEMENTARY NOTATION: The work reported herein was performed under Subcontract 85-038 to the Center for Space Engineering.

17. COSATI CODES		
FIELD	GROUP	SUB. GR.

18. SUBJECT TERMS (Continue on reverse if necessary and identify by block number): MEM, maximum entropy, autoregressive interferograms, Fourier

19. ABSTRACT (Continue on reverse if necessary and identify by block number)

This report is an evaluation of an Autoregressive (AR) method of spectral estimation, which has been incorporated into an interactive software package designed specifically for processing interferograms. The evaluation of this method of spectral estimation is based on a comparison of AR spectral estimates with those of a conventional Fourier transform method. The principle conclusions from this evaluation are: 1) that for high SNR this AR method offers significant advantages in resolution of low line density spectra which could permit shortening the interferometer drive length by at least a factor of three, and 2) for high line density spectra and high SNR one may achieve a factor of two over Fourier methods because it is not necessary to apodize the interferogram.

20. DISTRIBUTION/AVAILABILITY OF ABSTRACT	21. ABSTRACT SECURITY CLASSIFICATION
UNCLASSIFIED/UNLIMITED ☒ SAME AS RPT. ☐ DTIC USERS ☐	Unclassified

22a. NAME OF RESPONSIBLE INDIVIDUAL	22b. TELEPHONE NUMBER (Include Area Code)	22c. OFFICE SYMBOL
Francis X. Robert	617 861-3641	LSP

DD FORM 1473, 83 APR EDITION OF 1 JAN 73 IS OBSOLETE.

Unclassified

SECURITY CLASSIFICATION OF THIS PAGE

Continued from block 11:
Interferograms

FOREWORD

As part of its commitment to national defense, the United States Air Force (USAF) supports investigations into the chemistry and physics of upper atmospheric energy dynamics. The Center for Space Engineering (CSE), at Utah State University, under Contract F19628-83-C-0056 with the Air Force Geophysics Laboratory (AFGL), assists in these investigations.

CSE awards subcontracts to various industrial and academic entities to assist with instrumentation production and data reduction/analysis. Under CSE subcontract no. 85-038, the Space Data Analysis Laboratory located at Boston College, MA, analyzed Michelson interferometer data obtained from various rocket-borne experiments.

As part of their work, Boston College scientists developed computer algorithms to obtain superresolution spectral estimation from Michelson interferometer data. This report describes the autoregressive (AR) methods of spectral analysis, compares the AR methods to Fourier transform methods, and gives conclusions from Boston College's research in this area. Boston College's software package (a magnetic tape) complements this report; CSE retained a copy of the tape in our archives for reference. CSE Document Number CSE/86-109 entitled, "ARSPEC: A Program for High Resolution Spectral Estimation from Interferograms" is the software description and user's manual for this software.

Unless otherwise specified, all work reported herein was performed by Space Data Analysis Laboratory at Boston College under subcontract to CSE. This research study was authorized and funded by the Air Force Geophysics Laboratory's (AFGL) program "Laboratory Director's Fund" (LDF) as Project Number ILIR5F. The AFGL program managers for this effort were Messrs. Donald R. Smith and Anthony J. Ratkowski. The authors wish to express their gratitude to Messrs. Smith and Ratkowski for their support of this study, and for setting up several helpful meetings and discussions.

This page intentionally left blank.

SUMMARY

Boston College researchers developed an autoregressive (AR) data processing method to enhance the resolution of spectra derived from interferograms. They compared the MEM theory and their AR method to that of traditional Fourier methods. In addition, they created an AR-based computer program which includes routines for computing and graphically displaying the estimated spectra. Finally, Boston College researchers tested their AR method.

Theoretically, MEM may be more efficient than Fourier methods in decoding interferograms carrying information with different spectral distributions. MEM may also obtain more information about a narrow spectral range, yielding high precision values for a few spectral lines. Fourier methods, on the other hand, may be more efficient when an interferogram contains information on a discrete set of frequencies.

Boston College's AR software package consists of two basic components. The first component symmetrizes and filters an initial interferogram. The filtered interferogram becomes the "input interferogram" containing only the spectral band to be analyzed. The second component of the AR software package contains the AR algorithm which computes the filter coefficients from the narrow band interferogram and then computes and displays the resulting AR spectral estimate. The AR software package provides high resolution graphic output, but does not compute values of estimated wavenumber and amplitude.

Boston College researchers studied simulated interferograms to determine to what extent a high line density spectrum can be estimated from interferograms with a finite SNR, and what kind of resolution improvement can be expected with low line density spectra. For high line density spectra and high signal-to-noise ratios (SNR), Boston College's AR implementation of the MEM principle enhances the resolution twofold over Fourier methods. With low SNR and a noisy interferogram it is not possible to increase resolution as much as with high SNR measurements, yet it seems possible to achieve a resolution comparable to the Fourier estimate with significantly less data.

This page intentionally left blank.

TABLE OF CONTENTS

This page intentionally left blank.

LIST OF FIGURES

LIST OF FIGURES (Cont.)

LIST OF RELATED PUBLICATIONS

Zachor, A.S., D.S. Smith, A Study of the Maximum Entropy Method of Power Spectrum Estimation as Applied to Interferometer Data, Scientific Report No. 18, AFGL-TR-86-0162, Contract F19628-83-C-0056, Center for Space Engineering, Utah State University, Logan, UT, 84322-4140, 15 September 1986. ADA179403

Yap, B.K., Atomospheric Radiance Profile Codes, Scientific Report No. 19, AFGL-TR-87-0009, Contract F19628-83-C-0056, Center for Space Engineering, Utah State University, Logan, UT, 84322-4140, 17 September 1986. ADA179258

Fox, J.L., Studies of Infrared Aurorae, Scientific Report No. 20, AFGL-TR-87-0010, Contract F19628-83-C-0056, Center for Space Engineering, Utah State University, Logan, UT, 84322-4140, 03 November 1986. ADA179539

This page intentionally left blank.

INTRODUCTION

AR Methods for Spectral Estimation from Interferograms

In this report, Fourier spectroscopy refers to the spectral analysis of the sampled output of a Michelson type interferometer as it views a stationary source of radiation. In the process a beam of radiation is split and caused to interfere with itself, multiplexing a wide spectral band into a serial data stream called an interferogram. The spectrum is recovered by a Fourier cosine transform of this output data stream. In this appplication the interferometer functions as an information channel which codes the spectral information into the output data series, actually an autocorrelation series of the input spectrum. The Fourier series furnishes an orthogonal set of functions to efficiently decode the information in the autocorrelation series.

Maximum Entropy Methods (MEM) of spectral analysis were developed to enhance the resolution of spectra derived from short time series over that attainable by Fourier techniques. Since these non-Fourier methods initially grew out of attempts to spectrally analyze short data records, it may not be apparent why they should be beneficially applicable to interferometer data which, at least under controlled conditions, may be as long as is necessary for Fourier processing. In fact, Dr. Pierre Connes suggested, in response to a paper by Despain and Bell on enhancing spectral resolution from fixed length interferograms, given at the Aspen International Conference on Fourier Spectroscopy (1971), that there should never be any reason not to design an interferometer with a sufficient drive length to achieve any desired resolution. Dr. A.T. Stair responded to this by noting that in non-laboratory measurements, such as those flown on satellites, or where measurements of transient phenomena are concerned, there are definite constraints on the drive length that may be employed, and that it is important, after the fact to extract all the information possible from the data.

Although Fourier transforms have come to be automatically associated with the Michelson interferometer, it should be remembered that this is not the only possible way to decode the autocorrelation series. In fact, an alternative method of decoding the interferogram, using a different set of orthogonal functions yielding higher resolution, was proposed by Despain and Bell [14] at the Aspen Conference. While their method was valid in principle it seemed to be too sensitive to noise in the measurements to be employed easily and advantageously

to actual data. The autoregressive approach to recovering spectral information from an interferogram which is being proposed and studied in this report is primarily an algorithm to provide greater spectral resolution than Fourier methods. At this stage it is computationally more complex than the Fourier transform, and is also limited by measurement noise in ways that require further study. But we will show in this report that autoregressive (AR) modeling may be a useful tool in spectral analysis under certain experimental conditions, especially when used in conjunction with the better understood Fourier methods.

In the spectral estimation problem of any actual time series the assumption is made that the series represents a finite number of samples from an infinite series. In both Fourier methods and MEM or AR methods one has to extend the finite time series, though in different ways for Fourier and non-Fourier methods. In Fourier analysis one arbitrarily assigns a value to the unknown samples of the infinite time series (consistent with the assumption of stationarity), generally zero. This procedure, called windowing, introduces an inherent resolution limit that is proportional to the length of the original time series, and effectively models the finite time series with a set of harmonically related sinusoids truncated to the length of the windowed time series. This predetermines a set of discrete frequencies, or line positions, in the spectrum for which spectral information is to be obtained. The resulting spectral estimates are also subject to leakage errors, where part of the energy in any part of the observed spectrum is spread over the whole spectrum. Attempts to reduce the leakage by judicious windowing of the data sample results in further degradation of the resolution.

The trade-off between leakage effects and reduction of resolution constitute a fundamental constraint in achieving optimal spectral estimation using Fourier methods. The Maximum Entropy (minimum information) principle allows one to handle the unknown samples of the infinite time series as statistically unknown quantities; i.e. we avoid imposing any arbitrary values on these quantities. This leads to an autoregressive model of the time series which avoids windowing and the associated resolution problems.

The AR method presented here, and implemented in an accompanying interactive software package, is an attempt to extract certain information from the interferometer data that may not be accessible by Fourier processing. It has been indicated in the above discussion, and demonstrated many times, how MEM methods are capable of yielding more specific information from a short data

series on the precise location of a few spectral lines than Fourier methods. A rigorous explanation of this fact is beyond the scope of this report, but some insight may be provided by examining some basic information channel concepts due to Shannon [2], and adapted to the interferometer problem by Despain and Bell [1].

The capacity of an information channel is specified by the bandwidth of the signal, and the signal-to-noise ratio (SNR) of the channel by the formula:

$$C = V0 \log(1+SNR) \text{ bits/seconds} ,$$

where C is the channel capacity and V0 is the bandwidth of the signal. For an interferogram the units of time become units of distance, and the total information passed by an interferogram of length 2 X0 is:

$$I = 2\ X0\ V0 \log(1+SNR) \text{ bits} .$$

This formula expresses the facts that the total amount of information retrievable from an interferogram depends on a drivelength-bandwidth product, and on the SNR of the interferogram. The Fourier data reduction method is one way of decoding the information multiplexed by the interferometer into the interferogram, and it may be the most efficient method given data with certain characteristics. By modeling the data with harmonically related sinusoids the Fourier method effectively preselects a discreet set of frequencies about which information is to be obtained, and the interferogram would be most efficiently decoded if it contained information on only those frequencies. In some cases where the interferogram carries information with different spectral distributions MEM methods may be more efficient in decoding the interferogram. In particular MEM methods may allow one to obtain much more information about a narrow spectral range, yielding very high precision values for a few spectral lines.

1.0 THEORY OF AR PROCESSING

1.1 Fourier Spectral Estimation

The Wiener-Khinchin relationship is the basis of standard Fourier methods of spectral analysis. It states that if R(t) is the autocorrelation function of a random process

$$R(t) = \int_{-\infty}^{\infty} X(t)\, X^*(t-s)\, ds \tag{1}$$

then the power spectral density of the process, S(f), is the Fourier transform of the function R(t).

$$S(f) = \int_{-\infty}^{\infty} R(t)\, \mathrm{EXP}(-i2\pi ft)dt; \quad R(t) = R(-t)\ . \tag{2}$$

If the integral in Eq. (1) is to exist then X(t) must be a stationary random process. When Eqs. (1) and (2) are applied to digital time series, the integrals are replaced by sums. For a random process X(n), n=0,1,2,...,N-1:

$$\hat{R}(k) = 1/(N-1) \sum_{n=0}^{N-1} X(n)\, X(n+k) \tag{3}$$

$$S'(f) = 2 \sum_{k=0}^{N-1} R(k)\, \mathrm{EXP}(-i2\pi kt)\ . \tag{4}$$

In Eq. (3) $\hat{R}(k)$ is a biased estimate of the Autocorrelation function R(k), which is defined statistically as the expectation value, or ensemble average, of the product X(n)*X(n+k). Evidently, for a time series X(n), where n=0,1,2,...,N-1, R(k) may not be estimated for k>N-1. Also, it is clear that as k approaches N-1, the estimate R(k) becomes poorer as the "ensemble" of products becomes smaller. Finally, in Eq. (4), the fact that there is an upper limit to the number of autocorrelation values that may be estimated, i.e. k<N-1, implies a windowing of the autocorrelation function that appears in Eq. (2). Eq. (4) may be rewritten

$$S'(f) = 2 \sum_{k=0}^{\infty} R(k)\, W(k)\, \mathrm{EXP}(-i2\pi kf)\ , \tag{5}$$

where W(k)=0 for k>N-1, and W(k)=1 for $k \leq N-1$.

The resolution and leakage problems in Fourier methods results from the truncation of the sum in Eq. (4) or, equivalently, the windowing in Eq. (5). If S(f) in Eq. (2) is the true spectrum, expressed in digital form as

$$S(f) = 2 \sum_{K=0}^{\infty} R(k)\ EXP(-i2\pi kf) \ ,$$

then the spectrum $S'(f)$ in Eq. (5) is related to $S(f)$ by a convolution:

$$S'(f) = \int_{-\infty}^{\infty} \bar{W}(f')\ S(f-f')\ df' \ , \qquad (6)$$

where $\bar{W}(f')$ is the Fourier transform of $W(k)$.

The spectrum $S'(f)$ is a smeared version of the true spectrum. The exact correspondence between $S'(f)$ and $S(f)$ depends on the exact form of the window function. One of the basic requirements of classical Fourier methods is to choose the window function so that $S'(f)$ is a good estimate of $S(f)$ in some sense.

1.2 Maximum Entropy Spectral Estimation

Maximum entropy methods (MEM), as introduced by Burg [5], recognize that the windowing problem in Fourier methods results from arbitrarily setting the autocorrelation function in Eq. (4) to zero for $k > N-1$. The Burg approach, like the classical Fourier approach, begins with the Wiener-Khinchin relationship in Eq. (2), but avoids the necessity of setting the unknown values of the autocorrelation function to zero (or any other arbitrary value). It begins by asking what the best estimate of $S(f)$ in Eq. (2) is, given that we have no information about $R(k)$ for $k > N-1$, and formulates the answer mathematically in terms of the concept of information, or entropy.

Probability theory shows how to construct from the Wiener-Khinchin relationship a function of the autocorrelation coefficients, called the entropy, which is related to the amount of informaton available about these coefficients. The entropy per sample of a random process $X(n)$, with Power Spectral Density (PSD) $S(f)$, is defined as:

$$H = \int_{-f_N}^{f_N} \ln[S(f)]\ df \ ,$$

where f_N is the Nyquist frequency of the digital process $X(n)$. Or in terms of the Wiener-Khinchin relationship:

$$H = \int_{-f_N}^{f_N} \ln\left[\sum_{k=-\infty}^{\infty} R(k)\ \mathrm{EXP}(-i2\pi fk)\right] df \quad . \tag{8}$$

Maximizing the function H with respect to the R(k), for $k > N-1$ expresses our complete lack of information about these quantities, other than that they are consistent with the stationary samples we do know. This latter piece of information is incorporated into the analysis by the requirement that the inverse of Eq. (2)

$$R(k) = \int_{-\infty}^{\infty} S(f)\ \mathrm{EXP}(i2\pi kf)\ df \tag{9}$$

hold for the known autocorrelation values, for the spectrum S(f) that maximizes H. We thus solve the variational problem of maximizing the entropy relative to the unknown autocorrelation values, subject to the constraint of Eq. (9) for $k < N-1$. The solution to this problem is the spectral formula:

$$S(f) = \frac{P_M}{\left|1 - \sum_{K=1}^{M} a(k)\ \mathrm{EXP}(-i2\pi kf)\right|^2} \quad . \tag{10}$$

In the Burg formulation the a(k) are identified as the coefficients of a prediction error filter, or whitening filter. If $S(f) = |X(f)|^2$ then $\bar{X}(f)$ may be expressed from Eq. (10) as:

$$\bar{X}(f) = \frac{\sqrt{P_M}}{1 - \sum_{K=1}^{M} a(k)\ \mathrm{EXP}(-i2\pi kf)} \quad . \tag{11}$$

The denominator of Eq. (11) may be recognized as the transfer function of the time domain filter A, with a(1)=1. Then Eq. (11) may be rewritten in the time domain as:

$$A * X = \sum_{k=0}^{M} a(k)\ \ X(n-k) = e(n) \quad , \tag{12}$$

where e(n) is a white random process whose variance is the constant P. The a(k) in Eq. (10) are thus the coefficients of the whitening filter A, so called because the a(k) are determined from the process X(n) such that the filter transforms the X(n) into the white noise process e(n).

1.2.1 Autoregressive implementation of MEM principles

By writing the prediction error filter in Eq. (12) in a slightly different form:

$$X(n) = - \sum_{k=1}^{M} a(n)\, X(nk) + e(n) \qquad (13)$$

we see that X(n) is expressed as the output of an autoregressive process of order M, with the noise process as input. If a set of M coefficients a(k) can be found such that applying Eq. (12) to the actual time series yields a white noise series e(n), then X(n) is an autoregressive process where M is less than the number of samples available in X(n) then the MEM method may not be cpable of giving a satisfactory spectral estimate. If one does succeed in finding a set of coefficients that reduce a random process at least approximately to white noise then the spectral formula allows one to compute the PSD to infinite resolution from a finite set of coefficients. It is this feature that gives MEM methods their superesolution capability.

The application of the entropy principle to a random process has been rigorously formulated only for a Gaussian process leading to the entropy formula given above in Eq. (8). In this case the coefficients in the spectral formula correspond to the autoregressive process given in Eq. (13). Thus for a Gaussian random process the maximum entropy assumption leads to an autoregressive model of the time series. In the case of a high bandwidth, low information spectrum, modeling the interferogram with few autoregressive coefficients has two desirable features. First the spectrum exhibits high resolution resulting from the autoregressive spectral model. Secondly, while the autoregressive coefficients selectively model the information in the random process to high resolution they effectively smooth the noise. In Fourier processing any smoothing, as in Blackman-Tukey procedures, results in poorer resolution. This effect will be illustrated below in applying the AR method to a noise corrupted interferogram simulated from an OH spectral band.

1.2.2 Determining the coefficients of the autoregressive model

It is apparent that the essential requirement in implementing the autoregressive model is the determination of the autoregressive coefficients. These are the quantities a(k) in Eq. (13) or, equivalently, the prediction error coefficients in Eq. (10). One procedure is to relate the autocorrelation coefficients R(k) to the autoregressive coefficients. One may express the auto-

correlation coefficients of the process in Eq. (13) by taking the expectation values:

$$R(k) = E[X(n)\ X(n-k)]$$

$$= \sum_{\ell=1}^{M} a(\ell)\ E[X(n-\ell)\ X(n-k)] + E[e(n)\ X(n-k)] \ .$$

Now

$$E[X(n-\ell)\ X(n-k)] = R(\ell-k) = R(k-\ell)$$

$$E[e(n)\ X(n-k)] = P_M\ \delta_{k,o} \ .$$

In the second expectation value the Kroneker delta symbol indicates that the white noise in a process is correlated with the process only for the same time index. Therefore, the autocorrelation coefficients of the process in Eq. (13) satisfy the formula

$$R(n) = -\sum_{K=1}^{M} a(k)\ R(n-k) + P_M\ \delta_{k,o} \ . \tag{14}$$

For an autoregressive process of order M, and N samples in the autocorrelation series, the n(th) autocorrelation coefficient may be computed from the previous M coefficients using the M coefficients of the autoregressive model. Thus from a finite autoregressive model one may generate the infinite number of autocorrelation coefficients required in the Wiener-Khinchin relationship.

Remembering that $R(n) = R(-n)$, Eq. (14) may be expressed as a set of simultaneous equations, known as the Yule-Walker equations, in the following form:

$$\begin{aligned}
R(0) + a(1)\ R(1) + a(2)\ R(2) + \dots + a(M)\ R(M) &= P_M \\
R(1) + a(1)\ R(0) + a(2)\ R(1) + \dots + a(M)\ R(m-1) &= 0 \\
R(2) + a(1)\ R(1) + a(2)\ R(0) + \dots + a(M)\ R(M-2) &= 0 \\
\cdots\cdots\cdots\cdots\cdots\cdots\cdots\cdots\cdots\cdots\cdots & \\
\cdots\cdots\cdots\cdots\cdots\cdots\cdots\cdots\cdots\cdots\cdots & \\
R(M) + a(1)\ R(M-1) + \quad \dots\dots \quad + a(M)\ R(0) &= 0
\end{aligned} \tag{15}$$

If one has values of the autocorrelation coefficients, it is a straight-forward procedure to obtain the autoregressive coefficients by inverting the matrix of the autocorrelation coefficients. Representing the Yule-Walker equations in matrix form:

$$\begin{pmatrix} R(0) & R(1) & R(2) & R(M) \\ R(1) & R(0) & R(1) & R(M-1) \\ R(2) & R(1) & R(0) & R(M-2) \\ \cdots & \cdots & \cdots & \cdots \\ \cdots & \cdots & \cdots & \cdots \\ R(M) & R(M-1) & R(M-2) & R(0) \end{pmatrix} \begin{pmatrix} 1 \\ a(1) \\ a(2) \\ \\ \\ a(M) \end{pmatrix} = \begin{pmatrix} P_M \\ 0 \\ 0 \\ . \\ . \\ 0 \end{pmatrix} \qquad (16)$$

it is apparent that the matrix possesses a special diagonal structure, known as the Toeplitz structure. This makes it possible to invert the matrix using the Levinson algorithm which requires only on the order of M^2 computations, a very significant reduction of computation time over more general methods which require on the order of M^3 computations. This inversion thus remains computationally efficient for very large order matrices.

1.2.3 Processing interferograms by the AR method

The operational philosophy behind our modeling approach is different from that usually implemented in MEM spectra estimation. Typically one starts with a time series whose bandwidth is limited more or less to the low line density spectrum of interest. This time series is assumed to be a random process which can be satisfactorily represented by the inverse of a whitening filter of some order. One would then use the Burg algorithm to compute the filter coefficients from the entire time series, resulting in a model of the entire spectral band in the initial time series.

In computing spectral estimates from interferograms, the time series on begins with is an autocorrelation function whose lags are effectively an ensemble average over a large number of energy packets. In the case of an ideal noise free interferogram the problem of estimating an accurate autocorrelation function from a time series does not exist. However short the interferogram, there would be no reason not to compute the filter coefficients directly from the interferogram using the Yule-Walker equations. In practice, however, every interferogram will contain noise. Consequently, while the interferogram values are not statistically biased, they are subject to random errors. The significance of these errors for treating the interferogram as an autocorrelation function will depend on the signal-to-noise ratio in a manner that will be investigated empirically in this report.

The specific procedure presented here is designed to be implemented on an interferogram (autocorrelation series) associated with a broad spectral range, with the assumption that this broad spectrum may be partitioned into shorter "isolated" bands for analysis. Although no upper limit to the size of the band, in data points, has been established, better results tend to be obtained for more or less homogeneous bands of around 500 data points of less. A further advantage of using limited bands is that the resulting filter polynomial may be more readily factored to obtain the filter poles, and hence the line positions. This seems to be a more accurate procedure for finding line positions than a numerical search for peaks in the amplitude spectrum.

When a short spectral band has been selected for an analysis an interferogram containing only this band is filtered from the full symmetrized interferogram. The resulting interferogram will cover the same drive length as the initial data, but is sampled at a lower rate corresponding to the spectral range of the filtered band. Filter coefficients are then computed from this interferogram using the Yule-Walker equations as described above. The AR spectrum is computed from the formula in Eq. (10) using these coefficients, following some intermediate processing to insure that the displayed amplitude profile corresponds to estimates of the true line strengths.

2.0 DESCRIPTION OF INTERACTIVE AR SOFTWARE PACKAGE

The accompanying AR spectral estimation program consists of two basic components. This corresponds to the requirement that from an interferogram covering a wide spectral band, a narrow range must be selected for analysis in order to effectively utilize the capabilities of the method as implemented here. One component contains the AR algorithm which is designed to efficiently compute the coefficients of the whitening filter that is associated with the interferogram (autocorrelation function) as explained above, making use of the Levinson algorithm for inverting a Toeplitz matrix [11]. This component of the program also includes routines for computing and graphically displaying the estimated spectrum.

Algorithms have been included in this component of the program to process the raw AR spectrum in such a way that the relative amplitudes of the spectral lines are preserved. Absolute amplitudes of spectral lines are not preserved. This software presently contains no provision for radiance calibration, or for handling the effects of instrumentally caused apodization. The frequency axis may be scaled to wavenumber by specifying a constant sample rate. At the present state of development of this program there are no exact procedures to guarantee the quality of a particular spectral estimate, only very general guidelines for optimizing the quality of the estimates. This program is offered primarily as an analysis tool, and may in general have to be used along with other spectral estimates in order to achieve absolute measurement values.

The AR algorithm requires as input an interferogram containing only the spectral band to be analyzed. This "short" interferogram is obtained using support software contained in the other component of the total software package which is designed to symmetrize and bandpass filter an initial interferogram. Symmetrizing is accomplished with the Forman/Steele/Vanasse [12] phase filter approach, which approximately removes the linear phase distortion introduced into the interferogram by retidation offsets, as well as by other non-linear instrumental causes. The spectral selection is made from an apodized cosine transform of the symmetrized interferogram using graphic input.

2.1 AR Algorithm

The basis of this interactive AR software package is the algorithm that computes the filter coefficients from a narrow band interferogram and computes and displays the resulting AR spectral estimate. A narrow band "short" inter-

ferogram generated from the previously selected spectral band is read by the subroutine YULWALK which computes the filter coefficients. Given an interferogram R(n), of N points (lags), a set of N coefficients a(n,k) is obtained from the matrix equation (16) by a procedure originally due to Levinson (1947), and modified by Durbin (1960). Durbin's recursive procedure may be expressed as follows:

$$s(1)=R(0)$$

$$a(i,i) = -[R(i) + \sum_{j=0}^{i-1} a(j,i-1)\ R(i-j)]/s(i-1) \qquad (17)$$

$$a(j,i) = a(j,i-1) + a(i,i)\ a(i-j,i-1), \qquad 1 <= j <= i-1$$

$$s(i) = (1 - a(i,i)^2)\ s(i-1).$$

These equations are solved recursively for i=1,2,3,...,N if N is chosen as the order of the model. This procedure actually computes a set of coefficients a(i,j) for all model orders up to j=N, and the set of coefficients for order N are a(i,N). The array s(i) contains sigma values indicating the relative accuracy of the AR model for each order, with a(N) corresponding to P_M in equations (15) and (16). The raw AR spectrum is computed from equation (10) using the coefficients a(i,N).

As stated above the AR model of the spectrum is generally somewhat sensitive to the number of lags from the interferogram used to compute the coefficients. This number should, if possible be larger than twice the number of lines to be displayed in the spectrum, but not so large as to allow the noise to emerge in the spectrum. The user is allowed to select interactively the optimum number of lags from the available interferogram to achieve the best combination of resolution and amplitude stability in the displayed spectrum.

It is not generally useful to display the AR spectrum computed from Eq. (10) without further processing. In a Fourier spectrum the true amplitude is proportional to the integral over the fully resolved line, which is in turn a convolution of the true line shape with the scanning function. Since the scanning function modifies the shapes of all lines in the spectrum in the same way the relative amplitudes of the lines is preserved. In the AR spectrum computed from equation (10) the true line amplitude is also proportional to the integrated area under the line. However, the amplitude of the displayed line is

proportional to the square of the true amplitude, and in addition requires greater resolution to display than is generally convenient.

One way to represent the true line amplitude in this case is to integrate over the line in the AR spectrum and use that value to represent the line amplitude, ignoring the line shape. We have made use of this procedure and have found it accurate, but we have been prohibited by lack of time from developing it to the point where it will function easily in an interactive environment. Instead we have incorporated another procedure for obtaining line profiles in an AR spectrum which are estimates of the true line strengths. The AR spectrum displayed in this program is a convolution of the raw AR spectrum with a sinc squared line shape, whose resolution may be specified interactively in generating the display. Any other satisfactory line shape may be implemented as well, and it is usually possible to find a scanning function which leaves the lines narrow enough to be resolved in the displayed spectrum, while producing a line height proportional to the true amplitude. The line shapes in the resulting spectrum are very nearly those of the convolving function which essentially determines the resolution in the displayed spectrum, but the line amplitudes correspond to the true line strengths.

2.2 Supporting Software

2.2.1 Symmetrizing algorithm

Prior to the computation of the AR filter coefficients and spectrum, another component in this software package is employed to symmetrize the raw interferogram, and to generate a narrow band interferogram for the spectrum to be analyzed. The symmetrizing algorithm, based on the Forman/Steele/Vanasse method [12] computes a phase filter from a short selected length around the center of the raw interferogram. This is a low resolution filter having a complex spectrum of constant magnitude whose phase is the conjugate of that in the interferogram. A low resolution filter is used in this method because it requires relatively few additional points to the one sided interferogram, and because the phase of the raw interferogram is expected to vary only slowly.

2.2.2 Graphic selection of spectral range for AR processing

The narrow band interferogram is obtained by a Fourier transform from a limited range of the full cosine spectrum encompassed in the initial interferogram. The full cosine transform of the raw interferogram is displayed, and

the range desired for displaying in high resolution is marked out using a crosshair. In the selection process one may successively make expanded displays of several spectral bands before selecting the band for high resolution display. An interferogram of the selected band is computed by another cosine transform, and written out to a file to be accessed by the AR processing section of the program.

3.0 TESTS ON AR ALGORITHMS

3.1 Generating Synthetic Interferograms from Model Spectra

The development of this software was undertaken with the objective of achieving "super-resolution" spectral estimates of both low line density and high line density spectra from interferograms. We mean by a high line density spectrum one in which the number of spectral elements aproaches one half the number of data points available in the interferogram. This limit defines the capacity of the interferogram to carry spectral information. (In Fourier spectral analysis this corresponds to the full spectral range from zero to the Nyquist.) For an autoregressive model, in the ideal noise free limit, two lags (or interferogram points) are required for each two coefficients (or each pole) in the whitening filter, and hence for each spectral line. In this section of the report we present the results of studies on simulated interferograms to determine a.) to what extent a high line density spectrum can be estimated from interferograms with a finite SNR, and b.) what kind of resolution improvement can be expected with low line density spectra.

A low line density spectrum is one in which the number of points in the interferogram is much larger than twice the number of spectral elements. Given a sufficient SNR, a very significant increase in spectral resolution is expected for AR processing over that obtainable by Fourier methods for a low line density spectrum. This kind of result has often been reported in the literature with maximum entropy methods, and has been achieved in at least one case [6] with an interferogram of hundreds of data points, where there were less than ten spectral elements. Kawata et al. employed the Burg algorithm which treats the interferogram as a general time series. If the interferogram is sufficiently noise free, the Burg method unnecessarily limits the number of spectral elements that can be estimated from a given number of data points. The significance of these results lay in the resolution that could be obtained from an interferogram many times shorter (500 points) than would be needed with a Fourier spectral estimate (4000 points). It should be mentioned, however, that for interferograms with a poor SNR, where only a small percentage of the spectral information can be retrieved in any case, better results might be obtained with the Burg algorithm. For high line density spectra, the successful application of

the AR method appears to depend not only on noise level but also to some extent on the distribution of the spectral elements.

The studies reported here were made on simulated interferograms generated by direct Fourier transform from simulated spectra. Two spectra were simulated to test the performance of this software on low and high line density spectra. The high line density spectrum was a synthetically generated emission band of the molecule (CO_2), including 83 lines from 2300 to 2400 wavenumbers. The low line density spectrum that was used was part of the hydroxyl (OH) band. These spectra are shown in Figures 1a, and 7. For our purposes here the identification of the spectra is not important, except to establish some relevance of the tests to actual applications. Our procedure will be to compare the AR estimates of these spectra with Fourier estimates using the initial synthetic spectrum as a reference.

These spectra were used to generate interferograms of selected length and sample rate using a direct cosine transform. As a point of reference the approximate characteristics of a field widened interferometer [13] were adopted here (see figures 1b and 1c) in selecting sample rate and drive length, although the effects of some longer drive lengths were also investigated. A drive length of .56 cm for one side of the interferogram was simulated, and an effective sample rate of about 36000 samples/cm for the full band interferogram, or about 1.1 interferogram lags for each wavenumber in the spectral band of the interferogram. The final interferograms were generated by a Lorentz apodization of the cosine transforms to simulate a very narrow Lorentz spectral line shape, which is a better approximation to a physical line shape than the original pure sinusoid spectrum. Tests were made both with and without added noise. Added noise was white with a sigma specified in relation to the amplitude of the center of the simulated interferogram.

3.2 Line Matching Algorithm

In the following tests line position and amplitude comparisons were made between the value estimated in the AR model and the value for the corresponding line in the synthetic spectrum. For the Fourier spectrum line positions were determined by searching for peaks in the cosine transform of the interferogram. The search was initiated on a cosine spectrum interpolated by a factor of four, an effective wavenumber resolution of about .2, and the interpolation continued until a specified amplitude variation around the peak was met. In the AR case

the line positions were determined by finding the zeroes of the polynomial constructed from the filter coefficients [5].

Developing an algorithm to tabulate and plot these comparisons was complicated by the fact that in both the AR estimates and the Fourier estimates extraneous "lines" were generated. In the Fourier case these extraneous lines were due to sidelobes of the initial primary lines, and in the AR case they were identified with redundant poles in the filter. These redundant poles in the AR filter arise from using more than two autocorrelation values for each line in the estimated spectrum. It may be noted here that there is no a priori way to distinguish the extraneous lines generated by the redundant poles in the filter from the genuine lines in the spectrum being modeled. However, for a high SNR these poles will tend to lie sufficiently far from the unit circle to be distinguishable from those generated by the true spectrum, and for the extraneous lines to be invisible in a linear plot. For poor SNR these redundant poles will tend to model the noise, and this is responsible for the fundamental limitation in applying the AR method with a poor SNR. With a poor SNR the redundant poles may produce an effect similar to a phenomenon known as line splitting which has been associated with Burg method, the redundant poles in the AR model tend to distribute themselves uniformly around the unit cirlce instead of clustering about specific lines and producing true line splitting.

Because of these extraneous "lines" the algorithm had to be designed to select only those estimated lines that correspond to the original spectrum. In all cases where there was more than one estimated line for one line in the original spectrum the estimated line closest to the original line was selected. The primary output of this algorithm was a plot of wavenumber or amplitude deviation vs. wavenumber, presented along with a plot of the estimated amplitude vs. wavenumber. A sigma is computed for the wavenumber and amplitude plots to compare the rms deviations for the AR and Fourier spectral estimates.

3.3 Wavenumber and Amplitude Precision without Noise

3.3.1 Tests on CO_2

Fourier and AR spectral estimates were compared both with and without adding random noise to the interferogram. The comparison without noise was made in order to provide a benchmark to determine the degradation of the spectral

estimates for different noise levels, and also because an actual interferogram with high SNR could approach the ideal noise free case.

Tests on the application of AR modeling to high density line spectra were based on a synthetic spectrum of CO_2 provided by Atmospheric Radiation Consultants (Acton, Mass.), and was made available on an AFGL Cyber 750 computer permanent file. The spectrum consisted of the line positions and amplitudes of 82 CO_2 lines between 2300 and 2400 wavenumbers. The significant characteristic of this spectrum is that it consists of a P branch and an R branch, where the average line spacing in the P branch is somewhat greater than one wavenumber, while the average spacing in the R branch is somewhat less than one wavenumber. Figure 1 shows plots of the original synthetic "stick" spectrum of CO_2, along with an interferogram (autocorrelation series) of 128 lags generated from the synthetic spectrum by direct Fourier transform. Also shown is the interferogram obtained by band filtering a field widened interferogram (measured data) down to 128 points from the above 100 wavenumber CO_2 band. Note the similar drive lengths of the two interferograms.

A noise free interferogram of 128 lags was simulated from the CO_2 spectrum, which corresponded to the drive length and sample rate of the field widened interferograms. A Fourier processed spectrum, along with a plot of wavenumber differences between the original stick model and estimated spectra computed from this unapodized interferogram is shown in Figures 3. Examining a longer interferogram will illustrate more fully the relation-ship between a spectrum and the structure of the interferogram. Figure 2 shows an interferogram of 280 lags generated from the full synthetic CO_2 spectrum, along with interferograms generated from only the P and R branches. Note the appearance of two distinct "bursts" near the center of the interferogram of the full spectrum. Each of these bursts is centered at a drive length about equal to the inverse of the average line separation in the respective branch. Thus, in this case one could locate in the interferogram specific ranges where information associated with each branch of the spectrum was localized. It is now clear that the CO_2 interferogram of 128 lags used in this study effectively truncates the burst associated with the R branch of the spectrum. This implies that much of the information associated with the R branch has been lost in the shorter interferogram, and that no method of processing the interferogram will restore the detail in this part of the spectrum. According to the above definition of a dense spectrum, where the number of lines approaches half the number of lags

available in the interferogram, the CO_2 spectrum simulated here is overdense. that is, more information is being fed into the interferogram in this wavenumber band than its channel capacity will allow. This spectrum, therefore, provides an instructive example of how the AR spectral estimate responds to information in an overcrowded channel. The wavenumber differences for the P branch show a systematic deviation of the estimated wavenumber values from the correct values. Because the interferogram was not apodized the peaks represented in this cosine transform are distorted by the sidelobes of nearby lines. All further wavenumber and amplitude comparisons in this report will be based on triangularly apodized Fourier spectra, even though this may be accompanied by a degraded resolution. Note that the wavenumber deviations are not shown for the R branch of the spectrum. This is because the lines that appear in the estimated spectrum represent the original lines so poorly that it is difficult to find an unambiguous correspondence. Examining the interferograms in Figure 2, this absence of R lines is a result of having cut the interferogram off before the "burst" associated with the R branch of the spectrum. Consequently, there is not sufficient information in this interferogram to compute an accurate estimate of the R branch of the spectrum.

Figure 4 shows another Fourier spectral estimate using the same interferogram after it has been triangularly apodized. Only the peaks of those lines which are distinguishable have been resolved. However, the line position estimates are now extremely accurate, and show no systematic error. This is a clear illustration of the resolution limits imposed on Fourier spectral estimates by the necessity of controlling the effects of a finite data length by windowing.

As noted above, an interferogram does not require apodization when applying MEM spectral estimation. Figure 5 shows an AR spectral estimate using the same interferogram with no apodization. Here, all the lines in the P branch are clearly resolved with highly accurate line position estimates. The amplitude spectrum is distorted, however, with amplitudes of the lines toward the center decaying faster than in the original spectrum. This distortion of the spectrum is an effect of truncating the interferogram before the end of the burst associated with the P branch. By extending the interferogram farther into the burst from the P branch the amplitude profile of the AR spectrum of this branch is restored. Figure 6 shows the AR estimate using an interferogram with 164 lags, just twice the number of lines in the spectrum. The amplitude profile of the P branch has been approximately restored, and from the plot of wavenumber

deviations we see that some of the line positions at the lower end of the R branch are beginning to appear correctly.

In the CO_2 spectrum investigated the line spacing was such that the lines in the P branch could be fully resolved in a Fourier spectrum with no apodization. However, the lines in the unapodized Fourier spectrum were severely distorted by sidelobes, so that it is generally necessary to apodize the interferogram, which leaves some of the lines in the P branch unresolved. As a measure of comparison, one could claim at least a factor of two increase in resolution for the AR estimate for this high line density spectrum since this is just the resolution that must be sacrificed by apodization in order to obtain accurate line positions. This relative performance of the AR and Fourier methods for the CO_2 spectrum probably indicates what would generally be the case for high line density spectra where the information channel is effectively full.

3.3.2 Tests on Hydroxyl (OH)

The OH spectrum selected for this study was based on a set of 26 line positions and amplitudes between 3200 and 3600 wavenumbers shown in Figure 7. This low line density spectrum consists of a wide range of line spacings and amplitudes, and is the "made to order" situation for realizing the advantages of MEM methds in spectral estimation. A simulated interferogram having a drive length and sample rate as specified above consists of 445 lags for this wavenumber band. Fourier spectral estimates from this full interferogram with triangular apodization are capable of achieving full line resolution, and accurate line positions and amplitudes. The test in this case consisted in comparing the Fourier spectral estimates from the full interferogram with the AR estimate when the simulated drive length was reduced. This situation would arise in practice if one were forced to use an interferometer drive length too short for the required spectral resolution, or if it were necessary to limit the scan time to less than that required for a full scan.

It is pertinent to recall a point made above in discussing the theory of AR processing. When an AR model is used with a low line density spectrum the relatively small number of coefficients required in the model require correspondingly few lags from an interferogram. This results not only in the ability to obtain highly resolved spectra from relatively short interferograms, but also in an effective smoothing of the random noise in the spectrum. Thus, when a small

percentage of the total number of lags in a moderately noisy interferogram is used, the resulting filter coefficients selectively model the larger amplitude spectral lines, leaving the smaller noise spikes effectively smoothed. This smoothing is effective only if the amplitude of the spectral lines to be modeled are substantially larger than the noise spikes. If the noise amplitude is larger than the lines to be modeled, or if more than the minimum number of interferogram lags required to model the spectrum are used there will be a tendency for the noise to appear as spectral lines. One important implication of this fact is that the AR spectral estimate is actually degraded by using more than the optimum number of interferogram lags, although the range of optimality will generally be broad.

With a drive length and sample rate as specified above, the interferogram simulated from this OH spectrum contained 445 lags. Figure 8 shows the Fourier spectrum from the full interferogram, using triangular apodization. Also shown are plots of the errors in estimating the wavenumbers of the lines and the errors in estimating the amplitude profile. Since full resolution of all lines in this spectrum is obtained with an interferogram of this length, the line position and amplitude estimates are very accurate.

Figure 9 shows the AR spectral estimate of the same spectrum obtained using 150 (about one third) of the available lags from the interferogram. This spectrum is shown along with the wavenumber deviations of the line position estimates. Full resolution is obtained in this spectral estimate with only marginally poorer accuracy in wavenumber values and the amplitude profile. A Fourier spectrum using the same number of lags is shown in Figure 10, where it is seen that the group of four lines at the upper end of the spectrum is unresolved.

3.4 Wavenumber and Amplitude Precision with Noise

A comparison of AR and Fourier spectral estimates without noise is significant, even though no actual measurement can be noise free, because it constitutes a test of the theoretical limits of each of the two methods. However, a test of the practical effectiveness of these two methods should include a simulation of the noise inherent in any actual measurement process. Four sources of noise have been mentioned as having a possible effect on interferometer measurements [15]. These include detector noise, photon noise, scintillation noise and digitizing noise. Of these, photon noise and digitizing noise can be effec-

tively controlled by instrument and processing design. Scintillation noise depends on the object being measured and the surrounding environment, and is not readily characterized in a general way. Of these four sources, detector noise exhibits a fixed level in the measurement process, and will be of more significance in measuring weak signals than in measuring strong signals. Moreover, for practical purposes one may simulate this noise by a white random process. It is, therefore, possible and useful to investigate the effects of this kind of noise on the two measurement processes.

In recording interferograms, detector noise appears as random errors in the samples values of the interferometer output. One way to characterize the effect of these interferometer measurement errors on the spectrum is to express the noise corrupted spectrum as a sum of the true spectrum and a random spectrum, since the transformation is a linear one. That is, the total noise corrupted spectrum is the sum of cosine transforms of the noise free interferogram and a white random process. This shows that the effect of the white noise added to the interferogram is a broad band random spectrum. For a given total signal or energy in an interferogram, the effect of the noise component of the spectrum will depend on whether the energy in the interferogram is concentrated in a few lines or spread over a broad band. It is clear that in Fourier processing, a spectrum of a few discreet lines will tend to dominate the noise component.

The effect of random errors in the interferogram values on an AR spectrum is more complicated [10]. In computing the coefficients of the whitening filter from the Yule-Walker equations, there is an implied condition that the filter is stable. This will be true only if the interferogram corresponds to a positive definite spectrum [8]. Since this will not be true of a noise corrupted interferogram, by the above arguments, it is not possible to employ the Yule-Walker equations directly. In our tests we have employed a transformation designed to force the negative elements in the spectrum, assuming these are the effect of noise, to be positive. This transformation consists of computing a triangularly apodized cosine spectrum from the noise corrupted interferogram, and forcing all negative values to be positive, transforming back to an interferogram and removing the apodization. The Fourier spectrum corresponding to this new interferogram is effectively a positive definite random spectrum with about half the noise variance. We recognize that this interpretation of the procedure is

somewhat oversimplified, but the resulting AR spectra tend to confirm this interpretation.

3.4.1 Tests on CO_2

The noise figures in these tests are the random noise amplitude as a fraction of the amplitude of the zero lag of the interferogram. White noise of amplitude .05, or 5 percent of the zero lag of the interferogram was used in the CO_2 spectral estimates. This noise level seemed adequate to show the difference in the effect of noise on the Fourier and AR spectral estimates. Comparing Figure 12, showing the Fourier spectral estimate of the CO_2 band with the added noise, with Figure 4 the presence of the noise is clearly visible in the spectrum. The wavenumber estimates are poorest for the low amplitde lines at the low wavenumber end of the spectrum, but over most of the band are in errors are a small fraction of a wavenumber. The errors in the amplitude profile are distributed almost uniformly through the spectrum, averaging about seven percent of the maximum line amplitude. In Figure 13, the results for the AR spectrum compare favorably with relative to the no noise case shown in Figure 5. Again, the largest wavenumber errors are for the low amplitude lines, and are generally comparable over the whole P branch to the errors from the Fourier method.

3.4.2 Tests on Hydroxyl (OH)

The noise figure used in the comparison of the OH spectral estimates is .05, or 5 percent of the zero lag of the interferogram. Figure 14 shows the Fourier spectral estimate of the OH band. At this noise level there is a noticeable degradation in the precision of the wavenumber estimates over what was obtained with no noise (Figure 8) though, as would be expected, the larger errors occur for the smallest amplitude lines. Actually, the noise has prevented one pair of close lines from being resolved, as indicated by the small circle on the wavenumber plot in Figure 12. Inspection of Figure 7 shows a line at this position that is also present in Figure 8. With the noise this line was not adequately resolved from the adjacent line for the line matching algorithm to distinguish them. Also, where lines have been resolved, the amplitude estimates are only marginally poorer in the presence of noise than in the noise free case, with a sigma of .9 percent as compared to .1 percent.

Figure 5 shows the AR spectral estimate, again obtained from only 150 of the 445 lags. In this case the wavenumber estimates for the low amplitude lines are poorer than the corresponding Fourier estimates, although it should be noticed that the low amplitude line which was unresolved in the Fourier case has been detected here, with a resolution within one wavenumber. Even though these lines do not appear from the plot to be resolved, they appear as two distinct poles in the filter derived from the AR coefficients. The larger sigma for the wavenumber errors with noise compared to the Fourier estimate is due primarily to the poorer performance of the AR estimate for smaller amplitude lines. The error in the AR amplitude estimates of 6 percent of the amplitude of the largest line is poorer than that for the Fourier estimate, but it is still small.

It is a characteristic of the AR method that if one used many more lags than the minimum necessary to achieve full resolution (in this case around 150 lags) the performance in the presence of noise would not necessarily be improved. At approximately this number of lags the best compromise is achieved between modeling the true lines and smoothing over the noise in the spectrum. Using a much larger number of lags would tend to make the noise in the spectrum appear as additional spectral elements. This is one of the reasons why at this stage of development this AR method of spectral analysis may require some prior knowledge of the spectrum that is being observed.

3.5 AR Spectral Estimates from a Field Widened Interferometer

In this section of the report some AR spectral estimates obtained of a single interferogram from the field widened interferometer referred to above [13]. The data used here was measured by a rocketborne interferometer viewing vertically from a low altitude (about 86 km.). No attempt has been made to calibrate this data for wavenumber or radiance. The purpose of this analysis was to test the spectral estimation capabilities of this AR software on actual data. While we have chosen from this interferogram some of the same spectral bands that we simulated above, we have made no attempt to ascertain whether all of the same spectral lines are present in both, or whether the amplitude profile of the lines should be the same in both cases. In particular, the CO_2 spectrum used in the simulation was for an altitude of around 100 km, so that

the amplitude profiles from the simulated and actual data would not be expected to agree.

The AR estimates are shown for three spectral bands: NO from about 1720 to 2010 cm^{-1}, CO_2 from about 2274 to 2403 cm^{-1}, and OH from about 3185 to 3600 cm^{-1}. The corresponding apodized, interpolated, cosine transformed spectra are also shown for comparing amplitude profiles. The AR spectral estimate of the NO band is shown in Figure 16a, and the cosine transform spectrum is shown in Figure 16b. This is a high line density spectrum, with about 2.2 interferogram samples per spectral line in the P branch, and slightly less than 3 samples per line in the R branch. Although the cosine transform spectrum has resolved set of the P branch lines, they show more clearly in the AR spectrum. For this high line density spectrum the information band of the interferogram is nearly to full so both the Fourier type transform and the AR model should produce about equal results as a decoder of spectral information. The AR advantage is not needing to apodize the interferogram. This probably accounts for the better resolution in the AR estimate. The amplitude profiles of both estimates are comparable. Note the similar pattern in the larger amplitude lines of the P branch in both cases.

The CO_2 band is also a high line density spectrum. Without calibration there is no way of checking the line positions of the AR estimate, but the envelopes of both spectral estimates, shown in Figure 17, agree qualitatively even to the prominence of certain lines. Even though the R branch seems better resolved in this AR estimate the exact wavenumber values of the lines are suspect based on the interferogram shown in Figure 2, where the information in this branch is attenuated. It may be noticed from the lengths of the two interferograms in Figure 2 that the effective drive lengths for the simulated interferogram and the actual data appear to be about the same, implying similar Fourier spectral resolutions. The P branch in this AR spectral estimate is also very well resolved and the calibrated wavenumber values here should be accurate.

The AR estimate of an approximately 400 wavenumber OH band from the same intrferogram is shown in Figure 18a. In this case, as in the simulated case above for the same band, there is no evident improvement in resolution, but as in that case only about a third of the available interferogram was used to generate this spectrum. The corresponding apodized cosine transform spectrum is shown in Figure 18b. However, it is clear that we have basically duplicated the Fourier spectral estimate from a shorter interferogram. If we attempt to

greatly increase the resolution by taking more data from the interferogram we run into a processing problem of the reflection coefficients (the quantity a(M,M) in equations 2-1) becoming greater than unity. This is probably an effect of noise in the interferogram causing it to be a non-positive definite autocorrelation series. Although we have had some success in transforming this interferogram into one where the effect of the noise is reduced, as described above in section 3.4, this remains one possible area of development for this spectral estimation technique.

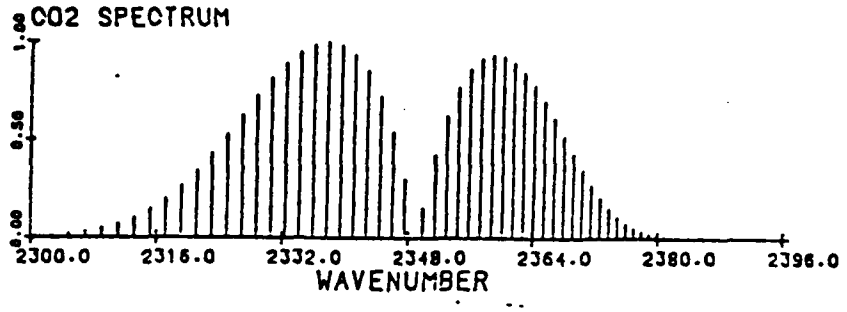

Figure 1a. "Stick" spectrum of CO_2 band showing P and R branches.

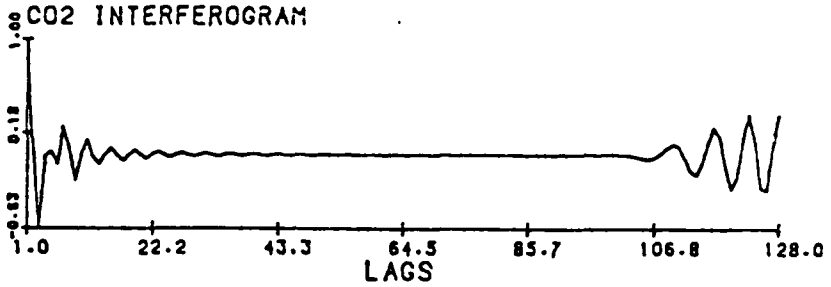

Figure 1b. Interferogram of 128 lags generated from CO_2 spectrum in Figure 1a.

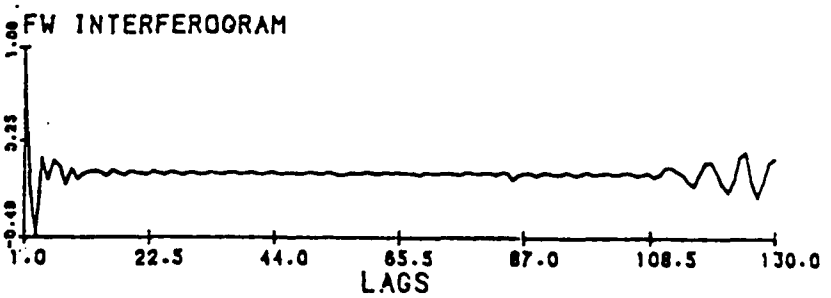

Figure 1c. Interferogram generated from 128 points of the CO_2 band measured by a field widened interferometer.

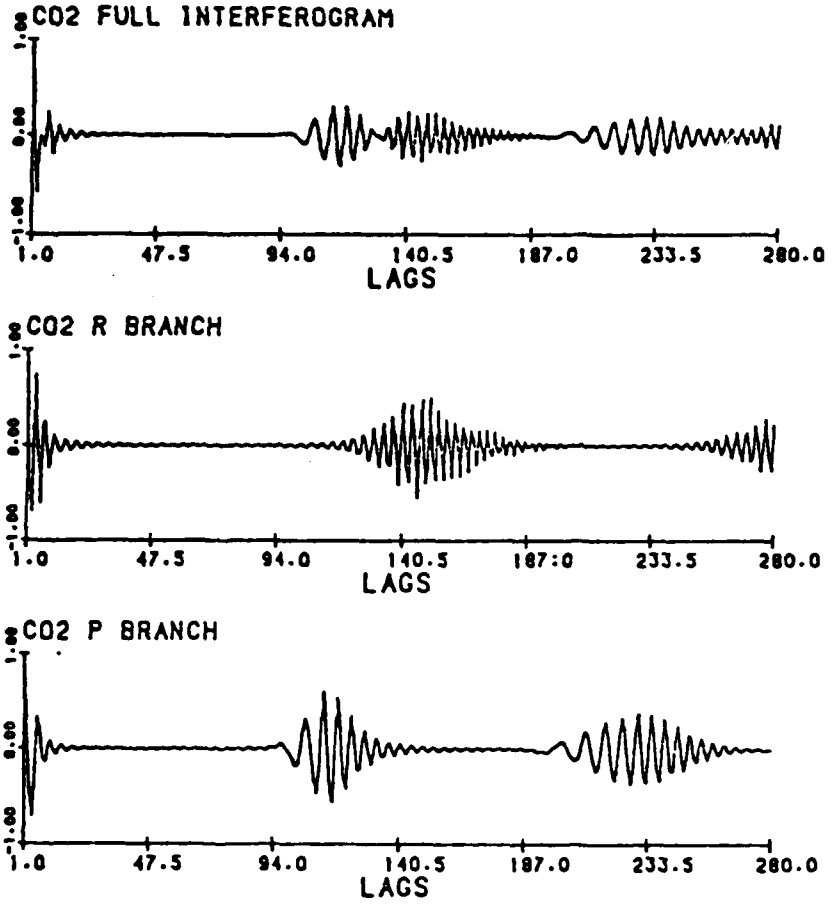

Figure 2. Interferogram generated from 2300-2400 wavenumber CO_2 band showing distinct contributions from P and R branches.

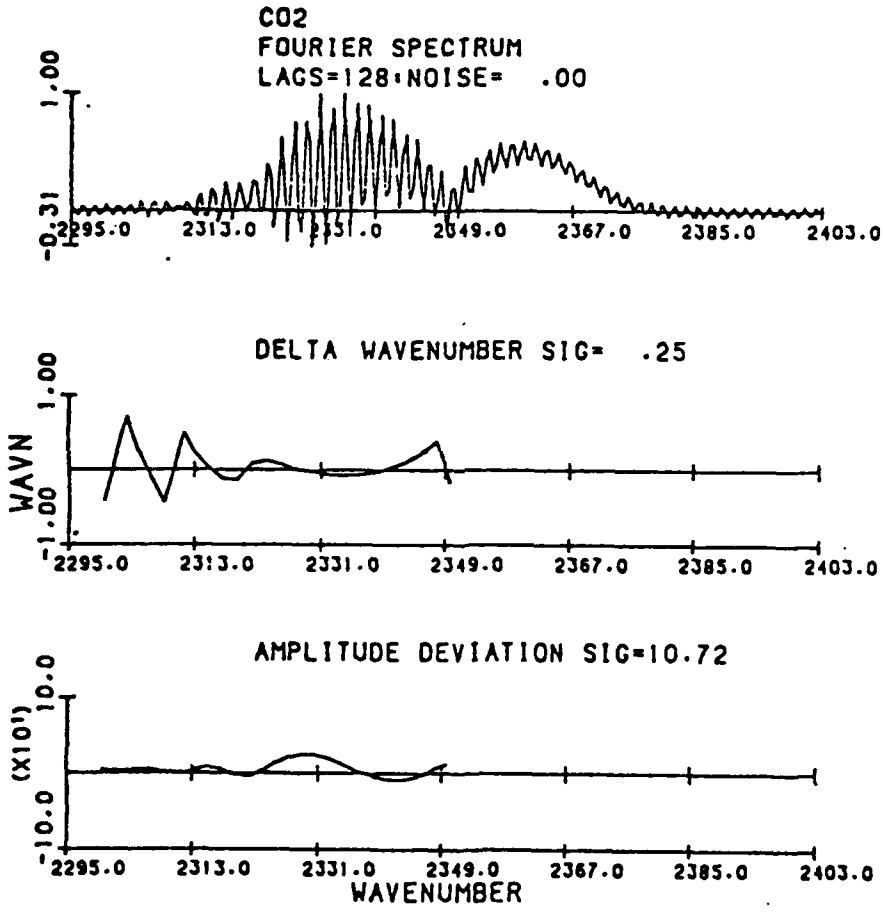

Figure 3. Fourier spectrum of 128 point unapodized interferogram generated from CO_2 spectrum. Also shown is a plot of the errors in the wavenumber estimates, and a plot of errors in the estimated amplitude profile.

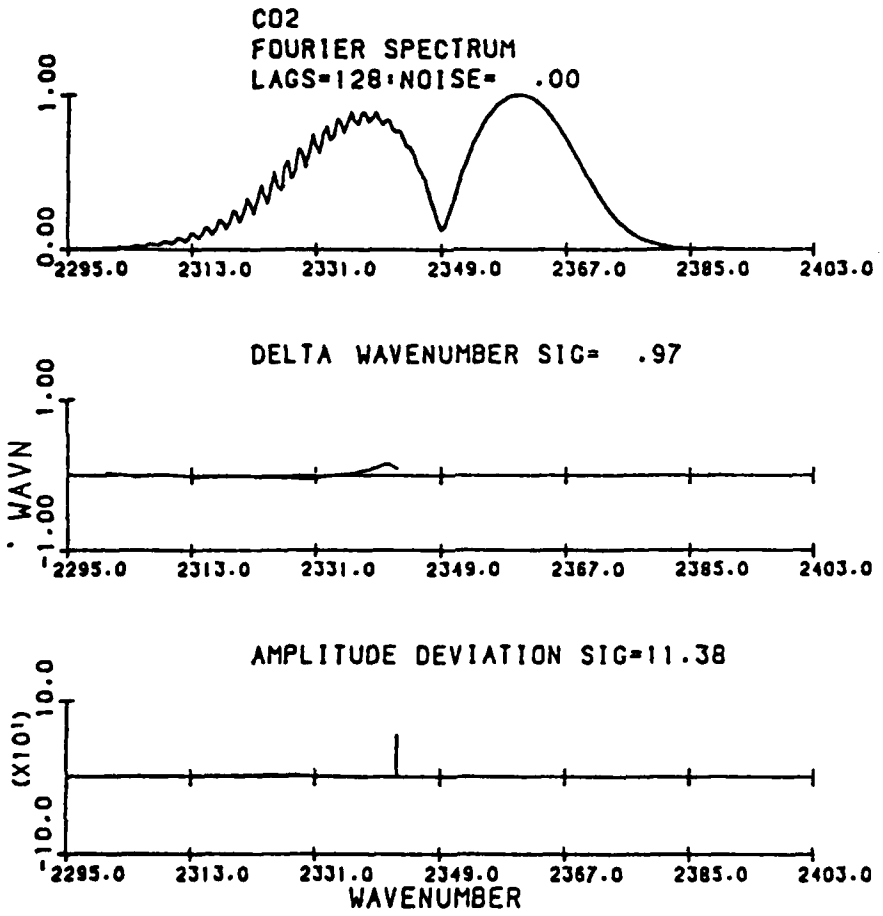

Figure 4. Fourier spectrum of apodized interferogram generated from CO_2 spectrum, with errors in the wavenumber estimates and amplitude profile estimate.

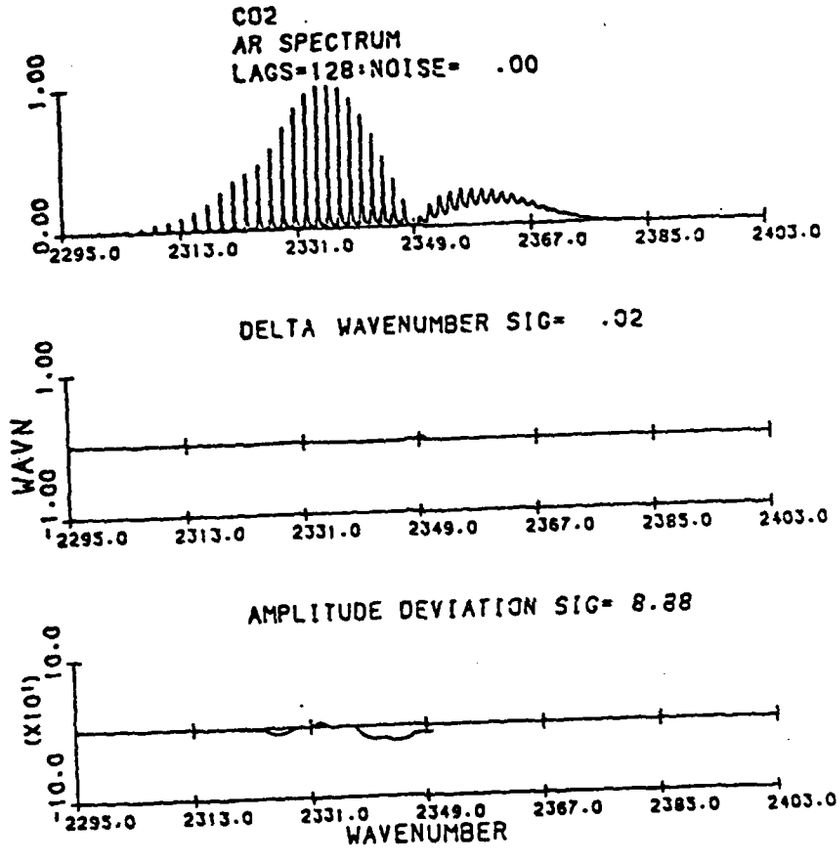

Figure 5. AR spectrum of unapodized interferogram generated from CO_2 spectrum, with errors in the wavenumber estimates and amplitude profile estimate.

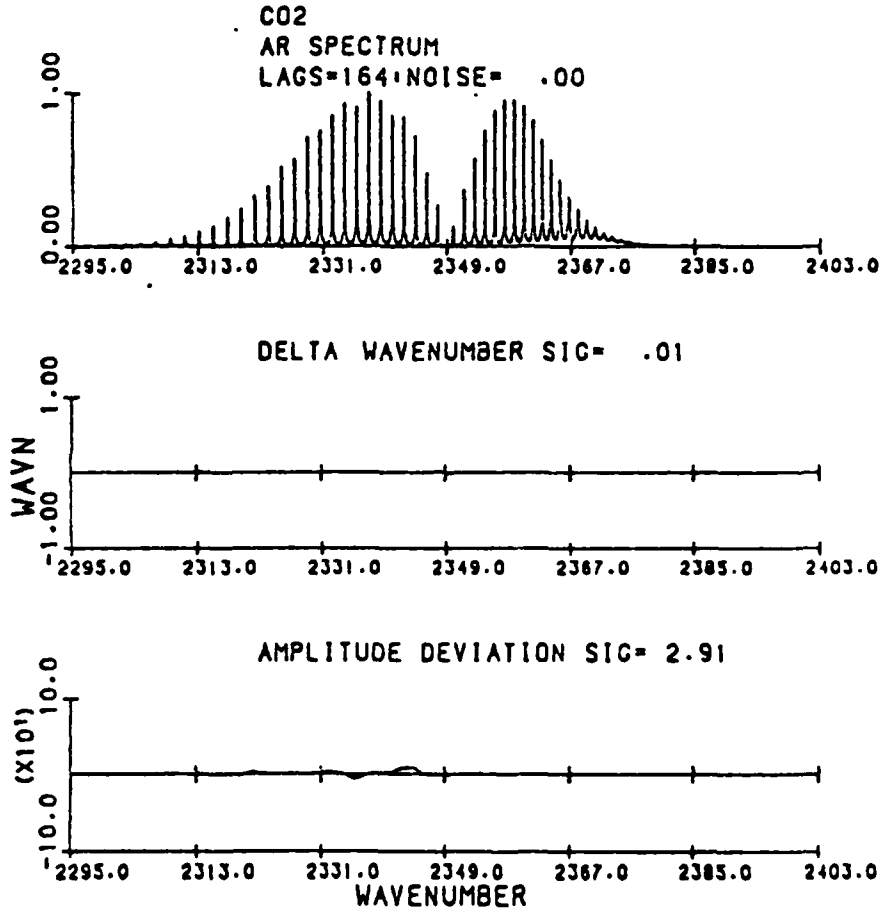

Figure 6. AR spectrum of unapodized interferogram of 164 lags generated from CO_2 spectrum, with errors in the wavenumber estimates and amplitude profile estimate.

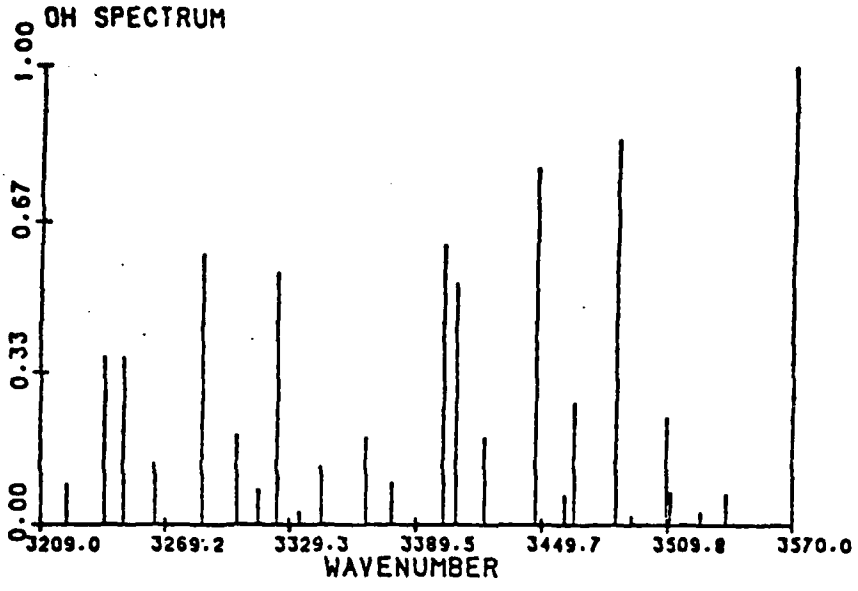

Figure 7. "Stick spectrum of OH band from 3200 to 3600 wavenumbers (after McDonald, et. al. [14])

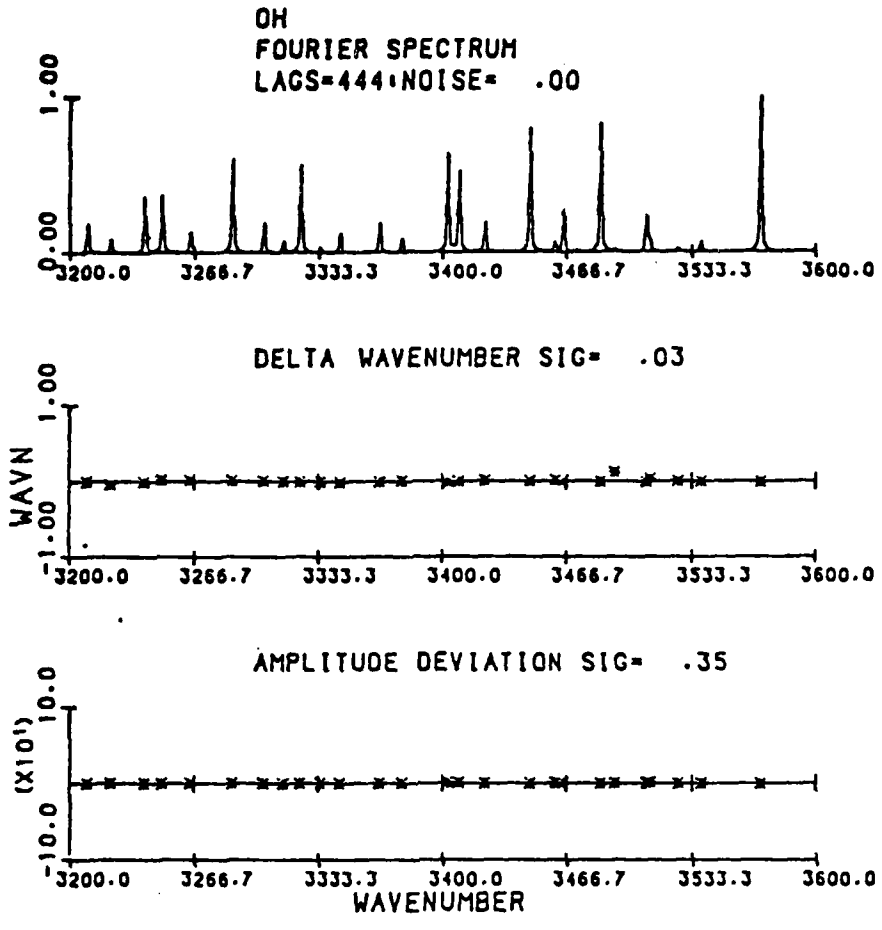

Figure 8. Fourier spectrum of 444 point apodized interferogram generated from OH spectrum. Also shown is a plot of the errors in the wavenumber estimates, and a plot of errors in the estimated amplitude profile.

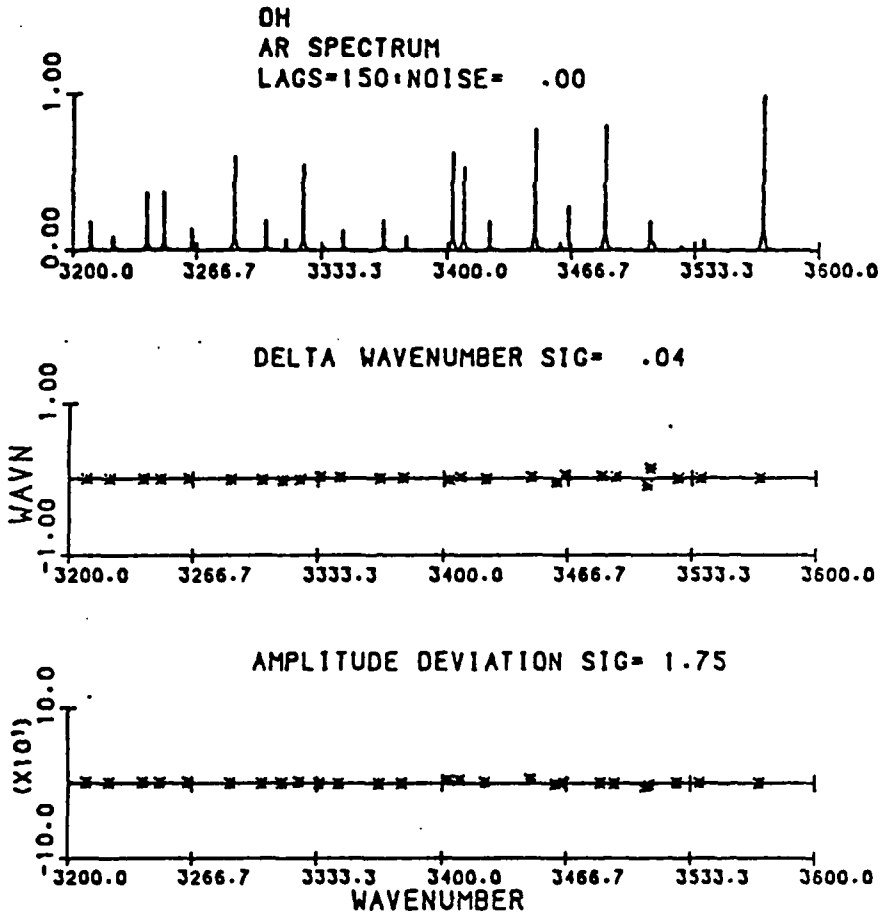

Figure 9. AR spectrum using 150 lags of the unapodized interferogram generated from OH spectrum. Also shown is a plot of the errors in the wavenumber estimates, and a plot of errors in the estimated amplitude profile.

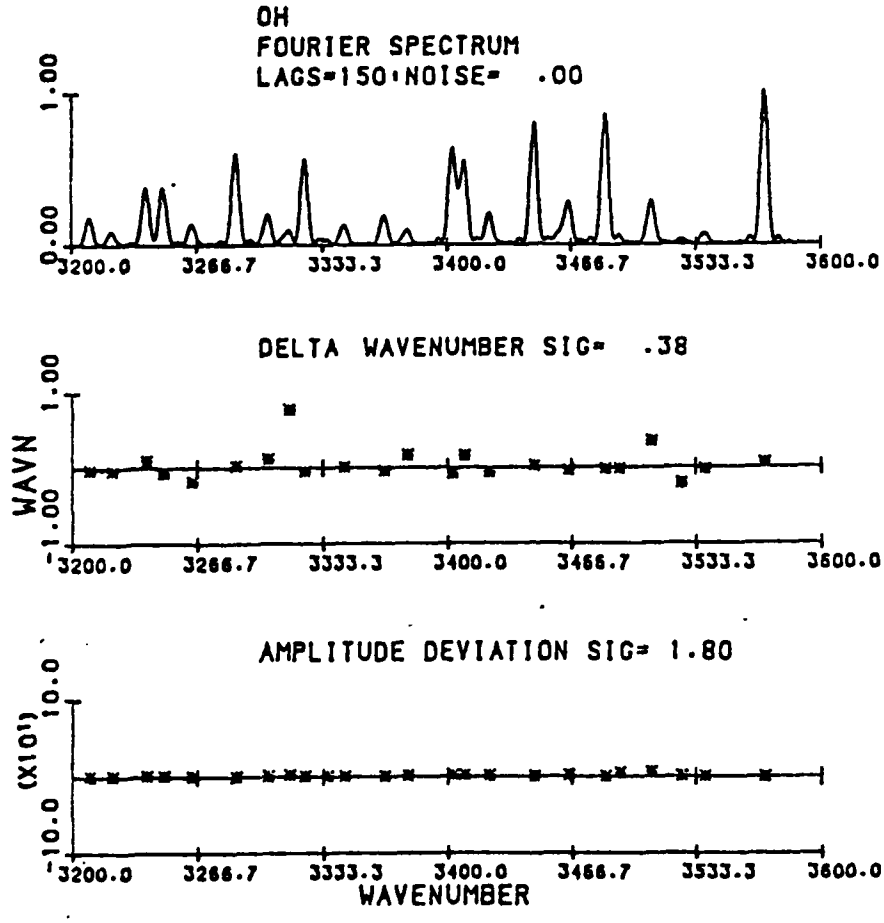

Figure 10. Fourier spectrum using 150 lags of the apodized interferogram generated from OH spectrum. Also shown is a plot of the errors in the wavenumber estimates, and a plot of errors in the estimated amplitude profile.

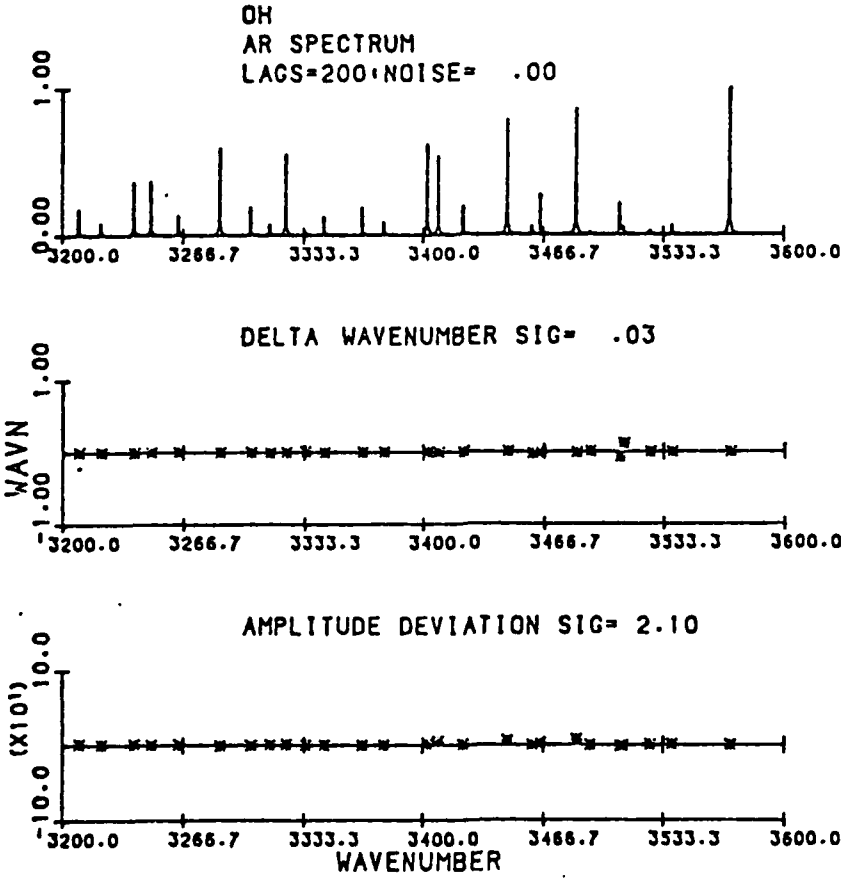

Figure 11. AR spectrum using 200 lags of the unapodized interferogram genertated from OH spectrum. Also shown is a plot of the errors in the wavenumber estimates, and a plot of errors in the estimated amplitude profile.

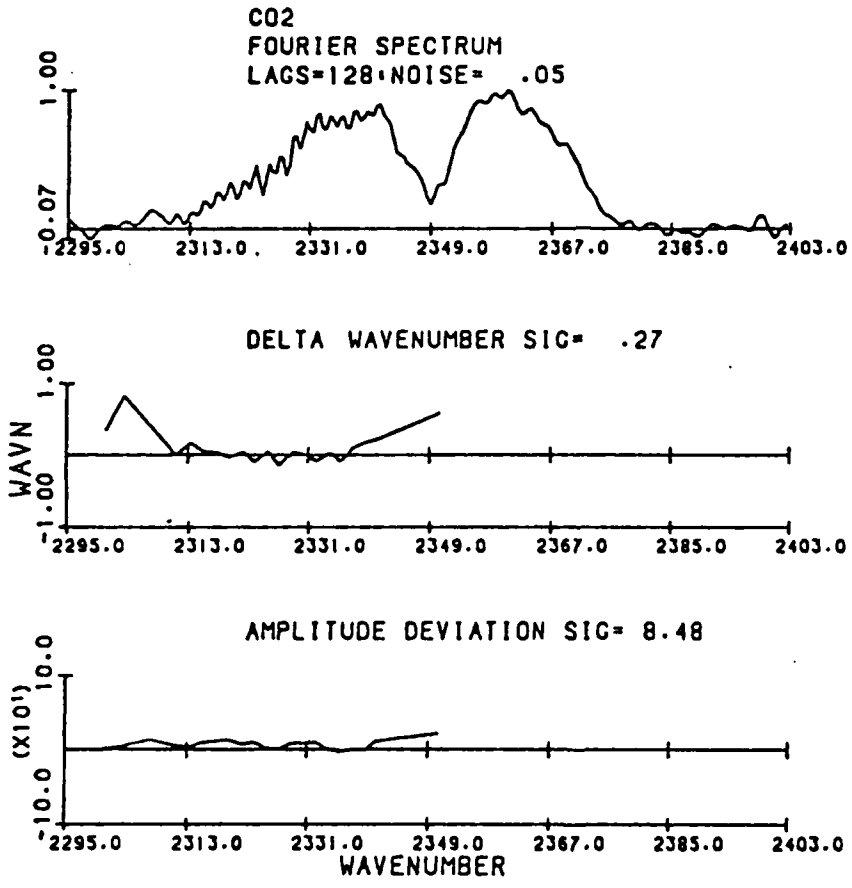

Figure 12. Fourier spectrum of 128 point apodized interferogram, with added random noise, generated from CO_2 spectrum. Also shown is a plot of the errors in the wavenumber estimates, and a plot of errors in the estimated amplitude profile.

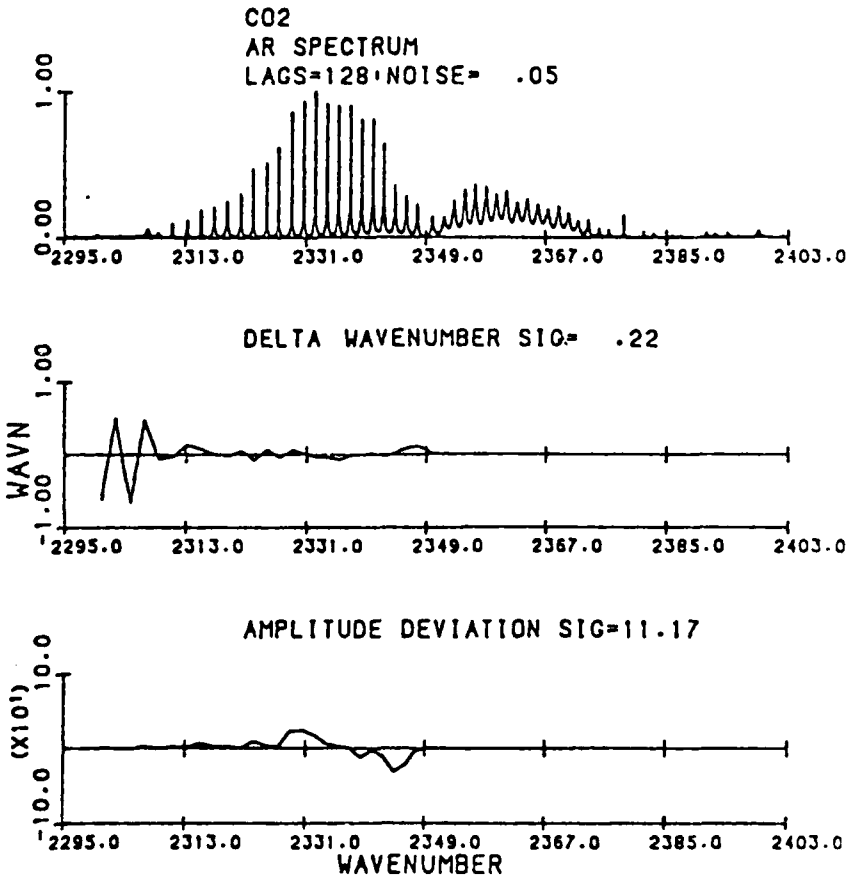

Figure 13. AR spectrum using 128 lags of the unapodized interferogram, with added random noise, generated from CO_2 spectrum. Also shown is a plot of the errors in the wavenumber estimates, and a plot of errors in the estimated amplitude profile.

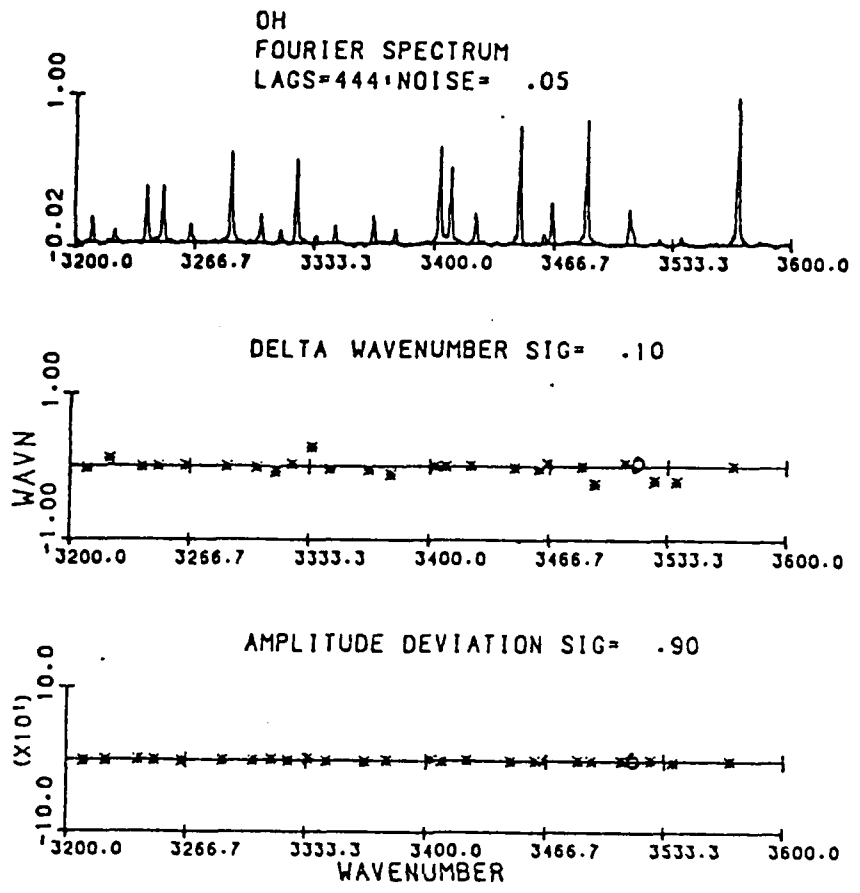

Figure 14. Fourier spectrum using 444 lags of the apodized interferogram, with a noise level of 5 percent of the first lag of the interferogram, generated from OH spectrum. Also shown is a plot of the errors in the wavenumber estimates, and a plot of errors in the estimated amplitude profile.

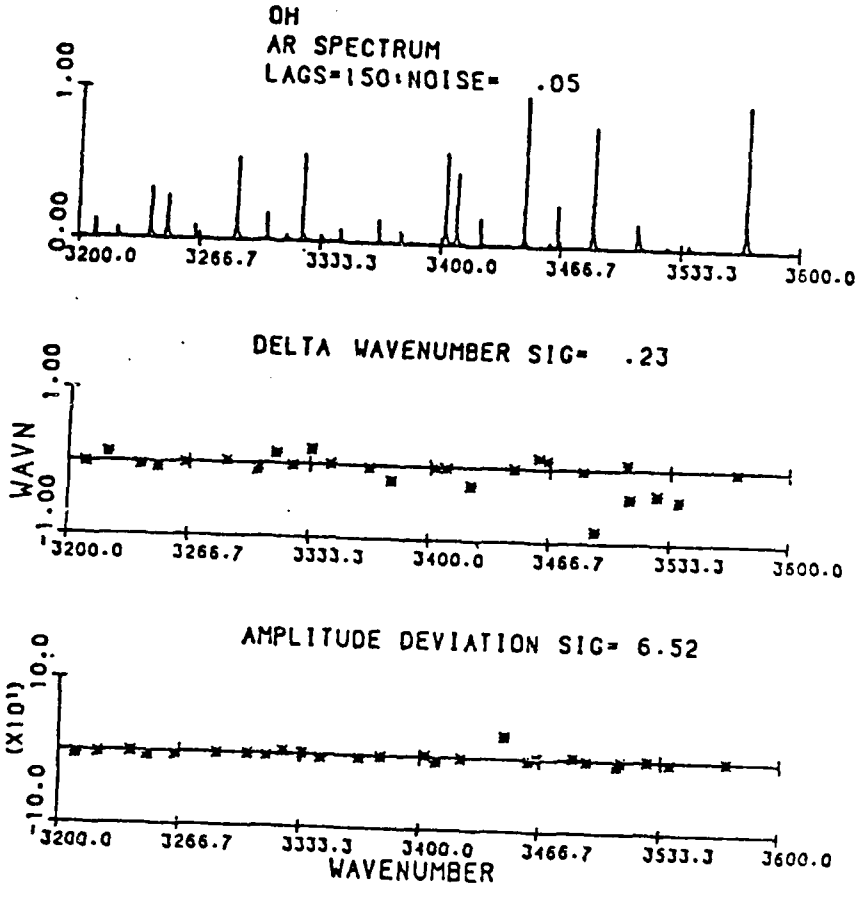

Figure 15. AR spectrum using 150 lags of the apodized interferogram, with added noise as in Figure 14, generated from OH spectrum. Also shown is a plot of the errors in the wavenumber estimates, and a plot of errors in the estimated amplitude profile.

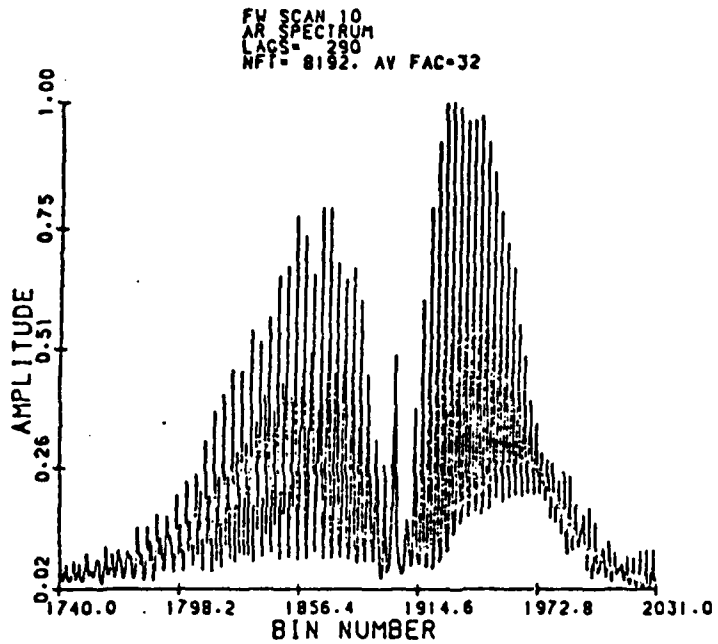

Figure 16a. AR spectrum of NO band - approximately 1715 to 2005 wavenumbers - from field widened interferogram.

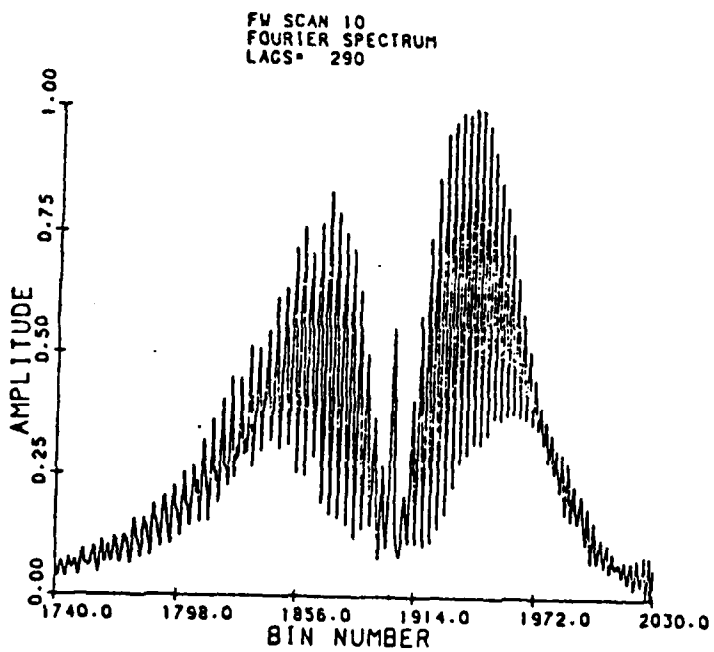

Figure 16b. Fourier spectrum of NO band, as in Figure 16a.

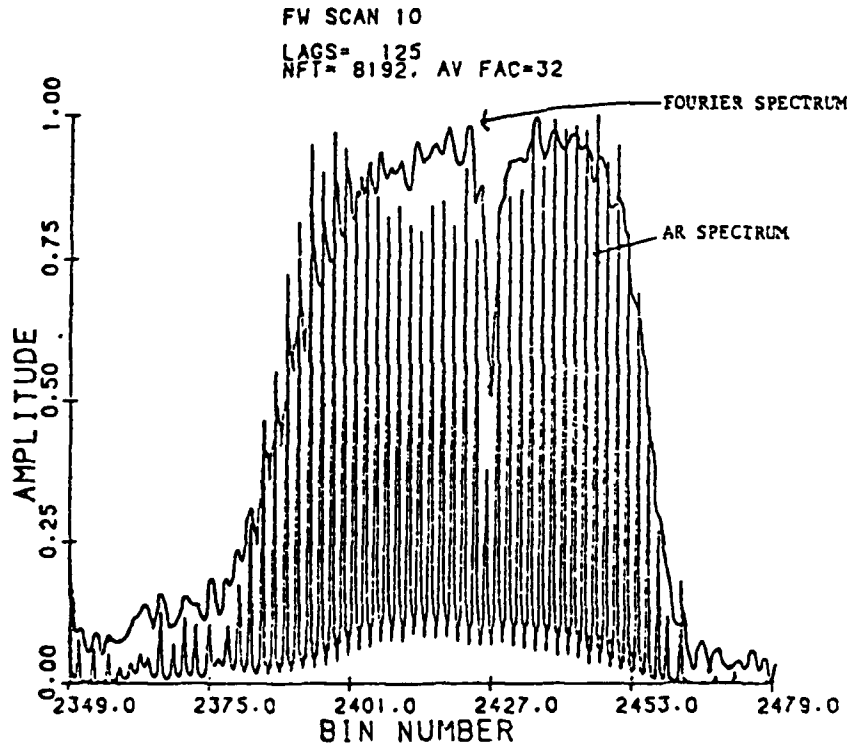

Figure 17. AR sectrum of CO_2 band - approximately 2275 to 2403 wavenumbers - from field widened interferogram. The Fourier spectral estimate from the same data appears as an envelope of the AR spectrum.

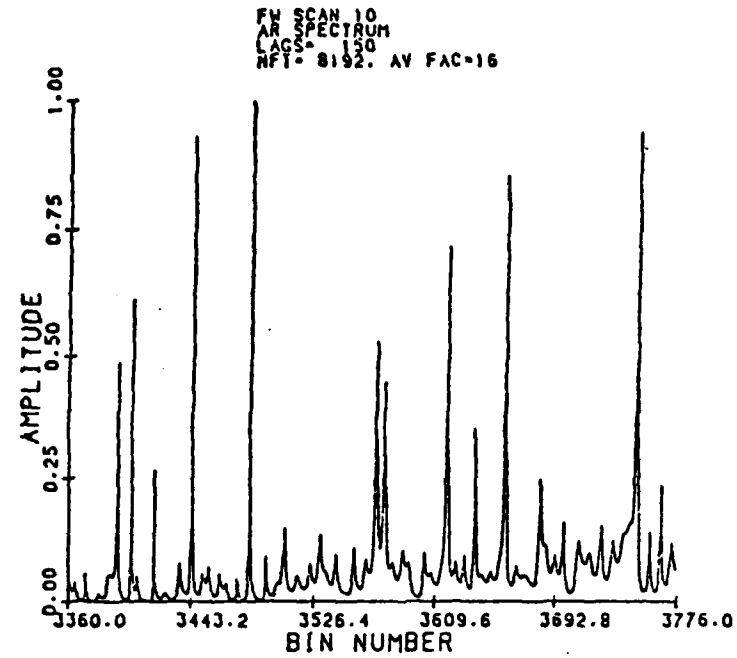

Figure 18a. AR spectrum of OH band - approximately 3200 to 3600 wavenumbers - from field widened interferogram computed from 150 out of 415 lags of the narrowband interferogram.

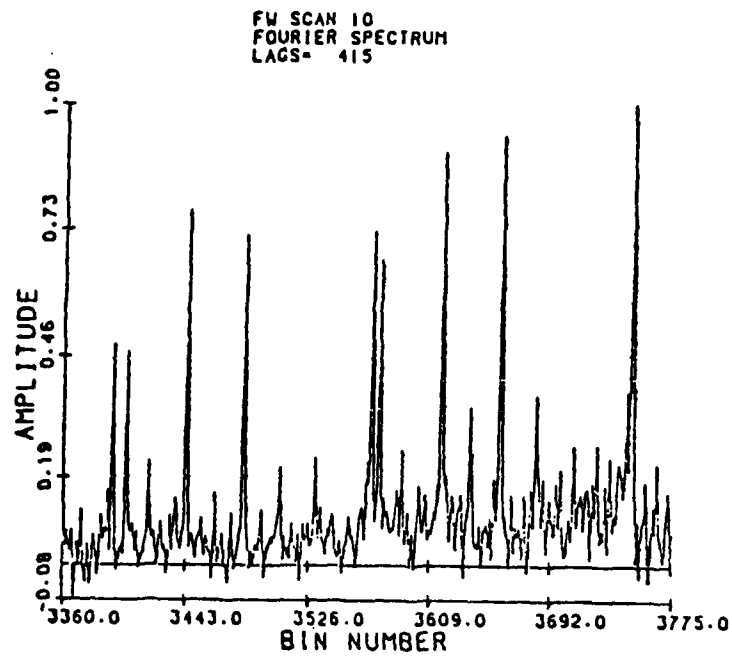

Figure 18b. Fourier spectrum of OH band, as in Figure 18a, using all available lags of narrow band interferogram.

CONCLUSIONS

This report is an evaluation of an Autoregressive (AR) method of spectral estimation incorporated into a high resolution interactive software package. It should be noted that, while the accompanying software package is capable of generating the AR spectral estimates as displayed in Figures 16 through 18, some of the results obtained in this report have utilized additional software which is not included in the interactive program. In particular, only graphic output is available from the interactive program at this time. The software which computed values of estimated wavenumber and amplitude values has not been incorporated in the interactive package. The time for this kind of software development was not available in this program, and our effort needed to be directed primarily toward testing the capabiliuties of the method itself rather than the existing interactive program. With these provisions, the results of the comparisons made in this report apply to the output of the interactive program.

The evaluation of the AR method of spectral estimation in this report is based on a comparison of this method with the results of the conventional Fourier transform methods. The Fourier results shown here for the simulated spectra were generally computed as cosine transforms of apodized interferograms generated from these spectra. The principal conclusions from these comparisons are as follows:

1. For a very high SNR, close to the no noise cases studied here, this AR method offers significant advantages in resolution of low line density spectra. This could be utilized, for the case of the OH spectrum studied here, for shortening the required drive length of the interferometer by a factor of two or three while still maintaining at least the line resolution and amplitude acuracy of the Fourier method. For high SNR it would also be possible to make use of additional interferogram samples to increase the resolution even further.

2. For high line density spectra and high SNR, the resolution enhancement of the AR method is limited because one is operating at the limit of the information carrying capacity of the interferogram. In this case one may still achieve a resolution improvement of at least a factor of two, which is what one loses by using a triangular or similar apodization to minimize line distortion due to sidelobes with the Fourier method.

3. Test with the simulated CO_2 spectrum indicated that with the added noise the degradation of the AR line position estimates appeared no

worse than the Fourier estimates. However, there did seem to be less accuracy in the amplitude estimates.

4. Conclusions on the AR spectral estimates of the low SNR simulated OH spectrum (low line density) may be more difficult to generalize. With a noisy interferogram it is not possible to increase resolution to the same extent as with high SNR measurements, since introducing more lags into the AR estimate, beyond those needed to model the basic signal, tends to amplify noise spikes instead of averaging over them. Nevertheless, it seems possible to achieve a resolution comparable to that from the Fourier estimate with significantly less data.

5. It should be recalled that it was necessary to pre-process the noise corrupted interferogram in order to implement the AR process, as described above. This was done to satisfy an inherent requirement in producing an AR model, that the reflection coefficient belonging to the set of filter coefficients from which the AR spectrum is computed be less than unity. This procedure was effective for the simulated spectra because it was possible to generate more lags than were needed. The effectiveness for actual data is more limited and we are studying alternate procedures for transforming a noisy interferogram to a positive definite autocorrelation series.

REFERENCES

1. Despain, A.M. and Bell, J.W., "Increased Spectral Resolution From Fixed Length Interferograms", Aspen International Conference on Fourier Spectroscopy, 1970 (Ed. Vanasse, G.A., Stair, A.T., Baker, D.J.), AFCRL-71-0019, 1971. AD724100

2. Shannon, C.E., and Weaver, W., "The Mathematical Theory of Communication", University of Illinois Press, Urbana (1949).

3. Durbin, J., "The fitting of time series models," Rev. Inst. Int. Statist., vol. 28, no. 3, pp. 233-243, 1960.

4. Levinson, N., "The Wiener RMS Error Criterion in Filter Design and Prediction," J. Math. Phys., vol. 25, no. 4, pp. 262-278, 1947.

5. Burg, J.P., "Maximum Entropy Spectral Analysis", Ph.D. Dissertation, Dept. Geophysics, Stanford Univ., Stanford, CA, May, 1975.

6 Kawata, S., K. Minauri, and S. Minami, "Superresolution of Fourier Transform Spectroscopy Data by the Maximum Entropy Method", Applied Optics, vol. 22, no. 22, Nov. 1983.

7. Kay, S.M., S.L. Marple, Jr., "Spectrum Analysis - A Modern Perspective", Proc. IEEE, 69, 1380-1418, 1981.

8. Makhoul, J., "Linear Prediction: A Tutorial Review", Proc. IEEE, vol. 63, 561-580, 1975.

9. Radoski, H.R., P.F. Fougere, E.J. Zwalick, "Comparison of Power Spectral Estimates and Applications of the Maximum Entropy Method", Journal of Geo. Res., 80, 1975.

10. Schott, J.-P., "Maximum Entropy Power Spectrum Estimation with Uncertainty in Correlation Measurements", IEEE Trans. Acoust., Speech, Sig., vol. ASSP-32, no. 2, April 1984.

11. Uhlrych, T.J., and T.N. Bishop, "Maximum Entropy Spectral Analysis and Autoregressive Decomposition", Rev. Geophys. Space Phys., vol. 13, pp. 183-200, Feb. 1975.

12. Forman, M.L., W. Howard Steel and G.A. Vanasse, Correction of Asummetric Interferograms Obtained in Fourier Spectroscopy, J. Opt. Soc. Am., 56,59 (1966).

13. Steed,, A., J.C. Ulwick, C. Harris, F. Cook, P. Straka, "Rocketborne Interferometer Measurements of SWIR/MWIR Spectra", Trans. AGU, vol. 64, no. 45, Nov. 1983.

14. McDonald, R., H.L. Buijs and H.P. Gush, "Spectrum of the Night Airglow Between 3 and 4 Microns", Can. J. Physics, vol. 46, 2575, 1968.

END

9-87

DTIC